Supplementary information for

Craniodental functional evolution in sauropodomorph dinosaurs

by DAVID J. BUTTON*, PAUL M. BARRETT *and* EMILY J. RAYFIELD

Contents

Other supplementary material for this manuscript includes:

Supplementary Data SD1: Taxon scores for measured biomechanical characters, body mass data, and ages.

Supplementary Data SD2: Full results from fitting single-rate models of evolution of craniodental and body mass evolution across 1000 dated trees.

Supplementary Data SD3: Results from fitting two-rate models of character evolution across 1000 dated trees.

Supplementary Data SD4: Results of fitting SURFACE models allowing for regime shifts in craniodental evolution across 100 dated trees.

Supplementary Data SD5: Results of fitting SURFACE models allowing for regime shifts in craniodental evolution across 100 dated trees, after the omission of poorly-known taxa.

S1. Taxon selection

Data were collected for all sauropodomorph taxa for which >20% of the aforementioned characters could be measured. Taxa known only from teeth were excluded, as was the *nomen dubium Astrodon*, as the referral of material to this taxon is based largely on assumed provenance (D'Emic, 2013). *Yimenosaurus* was also omitted as its phylogenetic position within Sauropodomorpha is currently unknown. *Panphagia*, *Eoraptor* and *Pampadromaeus* have been interpreted as basal sauropodomorphs (Martínez & Alcober, 2009; Cabreira et al., 2011; Martínez et al., 2011, 2013) or basal theropods/basal saurischians (Sereno et al., 1993; Martínez & Alcober, 2009; Ezcurra, 2010; Apaldetti et al., 2011, 2013, 2014; Cabreira et al., 2011; Martínez et al., 2013; Otero & Pol, 2013; McPhee et al., 2014). Whatever their relationships, they will be informative of the plesiomorphic sauropodomorph condition and were therefore included herein. Diplodocid skulls were classified after Whitlock (2011a) and Tschopp & Mateus (2013); however it should be noted that diplodocid cranial material can be very difficult to diagnose to species, or even genus, level (Tschopp *et al*. 2015).

This resulted in a sample of 67 taxa. The full taxon-character matrix is given in the supporting data SD1. Clade definitions as used in this study are given in table S1.

S2. Biomechanical character selection

Twenty-nine craniodental characters, which quantify the emergent functional properties of the feeding apparatus, were selected and measured from representative sauropodomorph taxa. This represents an expanded version of the dataset of Button *et al*. (2014), which measured only 20 characters and was restricted to Sauropoda. A comparison of the characters used herein with those utilized by Button *et al*. (2014) is given in table S2.

Clade	Definition	Source(s)
Sauropodomorpha (Huene 1932)	The most inclusive clade containing *Saltasaurus loricatus* but not *Tyrannosaurus rex*.	Taylor et al. (in press)
Plateosauria (Tornier 1913)	The least inclusive clade containing both *Plateosaurus engelhardti* and *Jingshanosaurus xinwaensis*.	Galton & Upchurch (2004)
Plateosauridae (Marsh 1895)	The most inclusive clade containing *Plateosaurus englehardti*, but not *Massopsondylus carinatus* or *Saltasaurus loricatus*.	Sereno (2007), Yates (2007a)
Massopoda (Yates 2007b)	The most inclusive clade containing *Saltasaurus loricatus* but not *Plateosaurus engelhardti*.	Yates (2007a, b)
Riojasauridae (Yates 2007b)	The least inclusive clade containing both *Riojasaurus incertus* and *Eucnemosaurus fortis*.	Yates (2007b)
Massospondylidae (Huene 1914)	The most inclusive clade containing *Massospondylus carinatus* but not *Saltasaurus loricatus* or *Plateosaurus englehardti*.	Sereno (2007)
Sauropodiformes (McPhee et al. 2014)	The most inclusive clade containing *Saltasaurus loricatus* but not *Massospondylus carinatus*.	McPhee et al. (2014)
Sauropoda (Marsh 1878)	The least inclusive cade including *Vulcanodon karibaensis* and *Saltasaurus loricatus*.	Salgado et al. (1997); Langer et al. (2010)
Eusauropoda (Upchurch 1995)	The least inclusive clade including both *Shunosaurus lii* and *Saltasaurus loricatus*.	Upchurch et al. (2004)
Mamenchisauridae (Young & Zhao 1972)	The most inclusive clade that includes *Mamenchisaurus constructus* but not *Saltasaurus loricatus*.	Naish & Martill (2007)
Neosauropoda (Bonaparte 1986)	The least inclusive clade containing both *Diplodocus longus* and *Saltasaurus loricatus*.	Wilson & Sereno (1998)
Diplodocoidea (Marsh 1884)	The most inclusive clade containing *Diplodocus longus* but not *Saltasaurus loricatus*.	Wilson & Sereno (1998)
Rebbachisauridae (Bonaparte 1997)	The most inclusive clade containing *Rebbachisaurus garasbae* but not *Diplodocus longus*.	Upchurch et al. (2004); Whitlock, 2011b.
Limaysaurinae (Whitlock 2011b)	The most inclusive clade containing *Limaysaurus tessonei* but not *Nigersaurus taqueti*.	Whitlock (2011b)
Nigersaurinae (Whitlock 2011b)	The most inclusive clade containing *Nigersaurus taqueti* but not *Limaysaurus tessonei*.	Whitlock (2011b)
Flgaellicaudata (Harris & Dodson 2004)	The least inclusive clade containing *both Dicraeosaurus hansemanni* and *Diplodocus longus*.	Harris & Dodson (2004)
Dicraeosauridae (Huene 1927)	The most inclusive clade containing *Dicraeosaurus hansemanni* but not *Diplodocus longus*.	Whitlock (2011b)
Diplodocidae (Marsh 1884)	The most inclusive clade containing *Diplodocus longus* but not *Dicraeosaurus hansemanni*.	Whitlock (2011b)
Diplodocinae (Janensch 1929)	The most inclusive clade containing *Diplodocus longus* but not *Apatosaurus ajax*.	Taylor & Naish (2005)
Macronaria (Wilson & Sereno 1998)	The most inclusive clade containing *Salatasaurus loricatus* but not *Diplodocus longus*.	Wilson & Sereno (1998)
Titanosauriformes (Salgado et al. 1997)	The least inclusive clade containing both *Brachiosaurus altithorax* and *Saltasaurus loricatus*.	Salgado et al. (1997)
Brachiosauridae (Riggs 1904)	The most inclusive clade containing *Brachiosaurus altithorax* but not *Saltasaurus loricatus*.	Wilson & Sereno (1998)
Somphospondyli (Wilson & Sereno 1998)	The most inclusive clade containing *Saltasaurus loricatus* but not *Brachiosaurus altithorax*.	Wilson & Sereno (1998)
Euhelopodidae (Romer 1956)	The most inclusive clade including *Euhelopus zdanskyi* but not *Neuquensaurus australis*.	D'Emic (2012)
Titanosauria (Bonaparte & Coria 1993)	The least inclusive clade containing both *Andesaurus delgadoi* and *Saltasaurus loricatus*.	Wilson & Upchurch (2003)
Lithostrotia (Wilson & Upchurch 2003)	The least inclusive clade containing both *Malawisaurus dixeyi* and *Saltasaurus loricatus*.	Wilson & Upchurch (2003)
Saltasauridae (Bonaparte & Powell 1980)	The least inclusive clade containing both *Opisthocoelicaudia skarzynskii* and *Saltasaurus loricatus*.	Wilson & Upchurch (2003)

Table S1: Clade definitions as used in this study.

Character	Character number in Button *et al.* (2014)
Continuous characters	
(C1) Gape length	C1
(C2) Anterior mechanical advantage	C2
(C3) Posterior mechanical advantage	C3
(C4) Jaw articular offset/jaw length	C4
(C5) Quadrate condyle length/articular glenoid length	C13
(C6) Maximum mandible height3/mandible length	C6
(C7) Average mandible height3/mandible length	C7
(C8) Upper toothrow length/skull length	C5
(C9) Lower toothrow length/mandible length	C5
(C10) Maximum symphyseal length/mandible length	C8
(C11) Symphysis angle	NA
(C12) Adductor fossa length/mandible length	C9
(C13) Supratemporal fenestra length/skull length	C10
(C14) Supratemporal fenestra breadth/skull width	C11
(C15) Temporal muscle angle	C12
(C16) External mandibular fenestra area/mandible lateral area	NA
(C17) Retroarticular process length/mandible length	NA
(C18) Premaxillary diverenge angle	C14
(C19) Tooth angle	C15
(C20) Tooth slenderness index	C16
Binary characters	
(C21) Heterodont dentition	NA
(C22) Denticulate dentition	NA
(C23) Recurved teeth	NA
(C24) Overlapping tooth crowns	NA
(C25) Tooth-tooth wear facets	C17
(C26) Interdigitating occlusion	C18
(C27) Precise occlusion	C19
(C28) Lateral plates	NA
(C29) Self-supporting tooth battery	C20

Table S2: Summary of the characters used in this study and the overlap with those employed by Button *et al.* (2014).

Similar studies have often focused on the mandible alone (e.g. Anderson, 2009; Anderson *et al*., 2011, 2013; Stubbs *et al*., 2013; MacLaren *et al*., in press) both to increase taxon coverage (Anderson *et al*., 2011, 2013) and due to potential compromise in signal from the skull due its multiple roles (Anderson, 2009; Anderson *et al*., 2011, 2013; Stubbs *et al*., 2013; MacLaren *et al*., in press). However, characters from both the skull and mandible were measured here, as the entire cranium was of interest in order to more fully capture feeding morphology, and to increase taxon coverage. A combination of 20 continuous metrics and nine binary characters

that show variation within Sauropodomorpha were measured. Although most disparity studies have focused on continuous metrics such combined datasets do have precedence (Anderson *et al*., 2011; Button *et al*., 2014). Characters were measured in ImageJ (Rasband 1997–2012, http://rsb.info.nih.gov/ij/) from a combination of personal photographs of fossil material and CT scan data where possible, and from figures in the literature; sources are given in the supplementary data. Measurements were performed in standard lateral view except where indicated otherwise, with the ventral edge of maxilla/dorsal edge of the dentary orientated horizontally.

Binary characters

(C1) Gape length

This character was taken as the length from the anterior tip of the toothrow to the jaw articulation, representing a measure of gape size (figure S1). This character was chosen over total skull length as it could be measured from either the skull or mandible in taxa preserving either element. Additionally, the size of the gape is more relevant to feeding behavior than overall skull length, and the two become relatively decoupled in sauropod taxa due to marked anteroventral rotation of the braincase in some taxa, especially in diplodocids.

Size is an important factor in feeding ecology. Gape size in herbivores dictates the maximum bite-size volume and the size of acceptable food items. Sauropodomorphs performed minimal oral processing (Christiansen, 1999; Upchurch & Barrett, 2000; Barrett & Upchurch, 2007; Barrett *et al*., 2011; Hummel & Clauss, 2011; Sander *et al*. 2011), with the loss of cheeks within Sauropoda cited as an adaptation towards increasing gape and permitting the use of the entire toothrow for cropping (Upchurch & Barrett, 2000; Barrett & Upchurch, 2007; Upchurch *et al*., 2007). As a result, bite volume would represent the primary constraint acting upon sauropodomorph feeding rate (Christiansen, 1999; Hummel & Clauss, 2011; Sander, 2011).

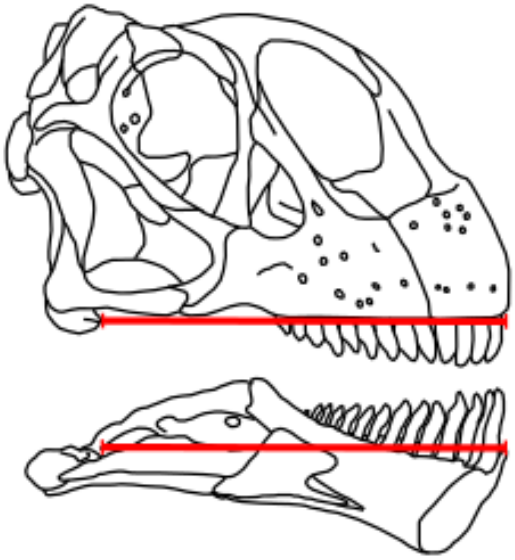

Figure S1: Illustration of the measurement of character C1, the gape length, demonstrated on the skull (lateral view) and mandible (medial view) of *Camarasaurus lentus*. From Button *et al*. (2014).

(C2) Anterior mechanical advantage

The mandible can be approximated as a third-order lever, with the input force (the pull of the adductor musculature) lying between the output force (exerted at the biting tooth) and the fulcrum (the jaw joint) (Hildebrand, 1982; Westneat, 1994, 2003; Wainwright & Richard, 1995). The efficiency of a jaw is hence described by the mechanical advantage (MA), the ratio of the inlever to the outlever (Westneat, 1994). The MA of a jaw is the inverse of the speed factor, so that the value of MA represents a trade-off between jaw closure power and speed (Westneat, 1994, 2003; Wainwright & Richard, 1995). Herbivores are freed from the necessity of a rapid, snapping, bite for prey capture, and so are generally expected to exhibit relatively high MA values versus faunivorous outgroups (particularly those carnivores that feed on small prey requiring no processing) (Hildebrand, 1982; Stayton, 2006). This is observed in lizards, where multiple herbivorous lineages show convergence towards greater MA values (Stayton, 2006).

However, it should be noted that vertebrate jaw action is more complicated in reality, involving variable activation patterns of multiple muscle groups (Gans, 1974; Westneat, 2003). Nevertheless, MA correlates with diet in extant fish (Westneat, 1994, 2003; Wainwright & Richard, 1995) and lizards (Stayton, 2006), and is commonly used in investigations of extinct animal feeding behavior (e.g. Janis, 1995; Anderson, 2009; Anderson *et al*., 2011, 2013), including those on archosaurs (Sakamoto, 2010; Stubbs *et al*., 2013; Button *et al*).

In- and outlevers were measured as parallel to the long axis of the jaw; with the vector of adductor muscle forces approximated as lying perpendicular to this line for the sake of simplicity. Although the moment arm from the jaw joint to the biting tooth will vary throughout the biting cycle a single measurement – in the horizontal position – was taken in order to avoid character tautology.

The inlever was measured as the distance from the articular glenoid to the midpoint of the area of attachment of the *m. adductor mandibulae externus* muscle group (figure S2a). This attachment site is present in sauropodomorphs along the dorsal edge of the surangular (Holliday, 2009); a smooth region marking the attachment of the *m. adductor mandibulae externus superficialis* is usually obvious in lateral view (Holliday, 2009). Inlevers for the *m. adductor profundus*, *m. psueudotemporalis* and *m. pterygoideus* groups (as in Sakamoto, 2010) were not measured. This was partially to avoid saturation of the character set with potentially interdependent characters relating to jaw shape, with the external adductor group chosen for mechanical advantage measurements due to its relative importance in Sauropodomorpha (Button *et al*., 2014). Additionally, the insertion sites for these other muscle groups are only visible in medial view, and so could not be reliably measured in specimens for which only lateral views of the mandible were available.

The outlever was then taken as the distance from the articular glenoid to the midpoint of the alveolar margin of the anteriormost biting tooth (figure S2a). This represents the longest outlever – and so the lowest MA – possible along the toothrow. This measurement was used rather than the distance from the glenoid to the tooth tip to permit evaluation in specimens with missing or damaged teeth.

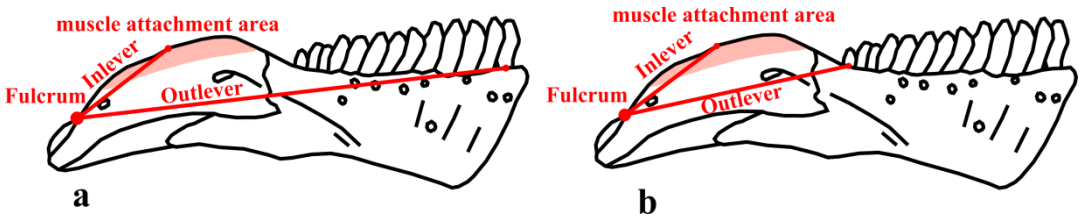

Figure S2: Illustration of character C2, anterior mechanical advantage of the mandible (a) and C3, posterior mechanical advantage of the mandible (b), on the jaw of *C. lentus* in lateral view. From Button *et al*. (2014).

(C3) Posterior MA

Conversely, the MA at the posteriormost biting tooth will represent the highest possible MA along the toothrow. For this character the inlever was identical to that of C2, with the outlever then measured as the distance from the articular glenoid to the midpoint of the alveolar margin of the final tooth (figure S2b).

(C4) Articular offset of the jaw/jaw length

An offset of the jaw articulation relative to the toothrow is commonly observed in herbivorous taxa (Janis, 1995; Reisz & Sues, 2000; Sues, 2000). This increases the leverage of the jaw muscles (Janis, 1995; Greaves, 1995) and simultaneous occlusion across the toothrow (Janis, 1995), as necessary for processing vegetation. An offset jaw joint is considered as indicative of herbivory in fossil taxa (Reisz & Sues, 2000; Sues 2000), and is also highly variable between sauropodomorph taxa (Upchurch & Barrett, 2000; Barrett & Upchurch, 2007).

To measure this character, a line was drawn level with the dorsal margin of the dentary. This was used, rather than a line level with the tooth apices, to allow inclusion of taxa preserving incomplete toothrows. The length of a line drawn perpendicular to this to the level of the articular glenoid was then measured (figure S3a). Finally, in order to correct for size, this length was divided by total mandibular length to yield the C4 value. In taxa lacking a preserved mandible an alternative but equivalent measurement was taken by projecting a line at the level of the ventral maxillary margin, and measuring the offset of the quadrate condyle perpendicular to this (figure S3b). This measurement was then divided by total skull length.

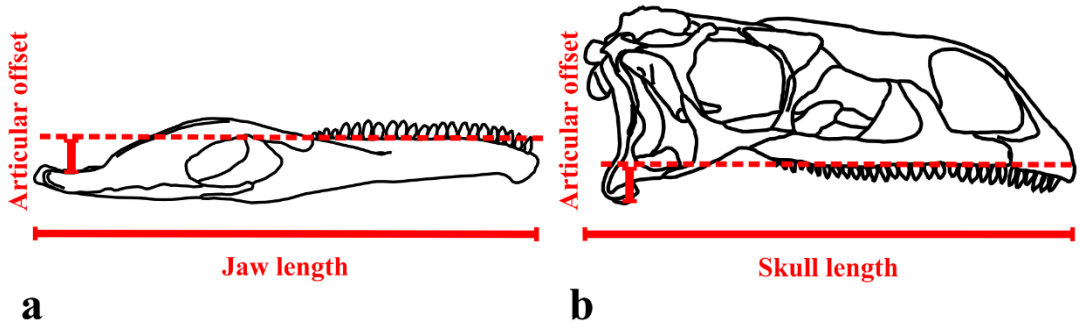

Figure S3: Illustration of the measurement of character C4, articular offset of (a) the mandible, and (b) the skull. The latter measurement was taken in instances where the mandible was not adequately preserved. Both illustrated using elements of *Plateosaurus engelhardti*.

(C5) Quadrate condyle length/articular glenoid length

Anteroposterior movements of the jaw (propaliny), permitted by an anteroposterior expansion of the articular glenoid relative to the quadrate condyle, are important in many herbivores (Reisz & Sues, 2000; Sues 2000). Diplodocids, in particular, exhibit marked elongation of the articular (Barrett & Upchurch, 1994; Upchurch & Barrett, 2000), and propaliny is inferred to have been important in 'branch-stripping' behaviors (Barrett & Upchurch, 1994; Upchurch & Barrett, 2000; Young *et al*. 2012).

Here, the anteroposterior length of the quadrate condyle was divided by the anteroposterior length of the articular glenoid to give a measure of the potential degree of propaliny (S4).

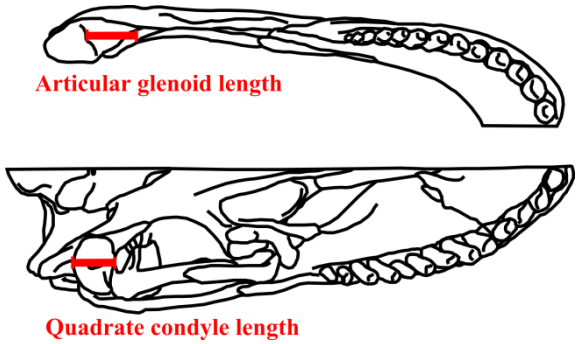

Figure S4: Illustration of the measurement of character C5, the ratio between the quadrate condyle length (bottom, illustrated on the skull of *C. lentus* in ventral view) and the length of the articular glenoid (illustrated on the mandible of *C. lentus* in dorsal view). From Button *et al*. (2014).

(C6) Maximum mandible height^3*/mandible length*

This character was used as a proxy for the second-moment of area (*I*) of the jaw, a measurement of the distribution of material about the centroid of a shape. The second-moment of area of the cross-section of a beam is proportional to its flexural rigidity (equaling the product of *I* and the Young's modulus of the beam material), and so deflection and induced stress under loading (Wainwright *et al*., 1976; Vogel, 2003). *I* has been used in functional studies upon multiple groups, including those on archosaurs (e.g. Metzger *et al*., 2005; Cuff & Rayfield, 2013). However, data on the cross-sectional area of the jaw are unavailable for most of the taxa in this study, many of which are figured only in lateral view. As the primary feeding-related forces will act upon the mandible in the dorsoventral plane, the height of the mandible can be used to derive a proxy measure for *I* (Anderson *et al*., 2013; Stubbs *et al*., 2013). However, it should be noted that ideally such a comparison would be made between jaws of similar mediolateral thickness (Anderson *et al*., 2013), so that, for example, the exceptionally thin cranial bones of *Nigersaurus* make this measurement potentially problematic for that taxon.

To derive this character, the maximum height of the jaw was taken and cubed, then divided by the mandible length (figure S5). It is noteworthy that this measurement is not size independent; nevertheless, size is an important factor in biomechanical performance and so this character was considered useful herein.

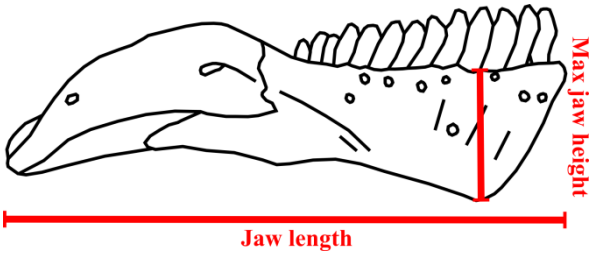

Figure S5: Illustration of the measurements taken for character C6, on the mandible of *C. lentus* in lateral view. From Button *et al*. (2014).

(C7) Average mandible height^3/mandible length

For this character the average height of the mandible (obtained by measuring the area of the mandible and dividing that by the length) was cubed and divided by the total mandible length, as above, to give a second proxy for *I*, as also used in Anderson *et al*. (2013) and Stubbs *et al*. (2013).

(C8) Upper toothrow length/skull length

The length of the toothrow dictates the tooth area available for cropping/processing. A longer toothrow will also exhibit more functional variance, with a range of MA across the jaw. A longer snout, and so toothrow, is thus important in faunivorous taxa requiring fast, weak, snapping bites for prey capture (e.g. Iordansky, 1964), but more forceful, slower posterior bites for dispatch/processing. Herbivores, particularly taxa exhibiting only limited processing, have more uniform requirements along the toothrow. Indeed, herbivorous taxa often exhibit relatively shortened snouts and toothrows compared with faunivorous outgroups (Reisz & Sues, 2000; Sues 2000).

However, although sauropods exhibit occluding upper and lower toothrows of equal length, the non-occluding dentitions of more basal sauropodomorphs typically exhibit significantly longer upper than lower toothrows. In order to maximize the data obtained and taxon coverage, the relative sizes of the upper and lower toothrows were recorded as separate characters. For character C8 the anteroposterior length of the upper toothrow was divided by the total anteroposterior length of the skull (figure S6a).

(C9) Lower toothrow length/mandible length

Character C9 is the anteroposterior length of the lower toothrow divided by the total length of the mandible (figure S6b).

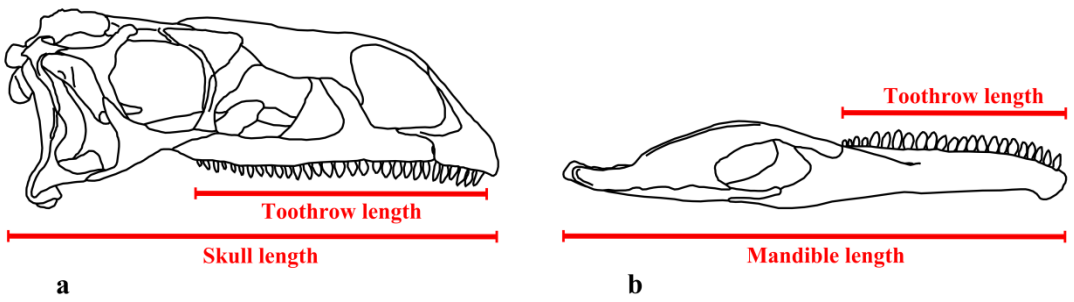

Figure 6: Measurements taken for character C8, relative upper toothrow length (a), and for C9, relative lower toothrow length (b), illustrated on the skull and mandible of *Plateosaurus englehardti*.

(C10) Maximum symphyseal length/mandible length

The mandibular symphysis needs to accommodate the range of bending, shear and torsional stresses incurred during different phases of the bite cycle (Hylander, 1984, 1985) different feeding behaviors (Walmsley *et al*., 2013) and in transferring forces from the working to the balancing side during unilateral biting (Porro *et al*., 2011). Sauropodomorphs are relatively conservative in terms of mandibular symphyseal morphology, with all taxa retaining the abutting, unfused plates plesiomorphic for archosaurs (Holliday & Nesbitt, 2013). However,

sauropods exhibit prominent dorsoventral expansion of the symphysis relative to more basal sauropodomorph taxa (Upchurch & Barrett, 2000; Barrett & Upchurch, 2007), which has been inferred to accommodate greater stresses as a result of a shift to bulk-feeding (Upchurch & Barrett, 2000).

Although the symphysis has to resist a variety of complex stress environments, its behavior can be predicted from relatively simple linear measurements (Walmsley *et al*., 2013). The maximum length of the symphysis was measured (after Anderson *et al*., 2013), and divided by total mandibular length (figure S7a). A caveat associated with this symphysis measurement is that the axis along which this length is measured is not identical in all taxa, due to differences in the symphysis angle (see below).

(C11) Symphysis angle

The angle of the symphysis was measured from a vertical line drawn perpendicular to the long axis of the jaw, defined as the plane of its greatest anteroposterior length when in the closed position (figure S7b).

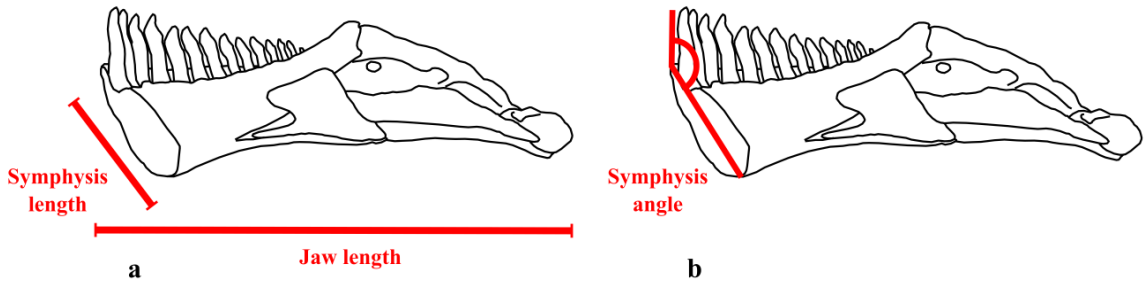

Figure S7: Illustration of the measurements taken for character C10, symphysis length:jaw length (a) and character C11, symphysis angle, shown on the mandible of *C. lentus*, in medial view.

(C12) Adductor fossa length/mandible length

The anteroposterior length of the adductor fossa was used as a proxy for the area of muscle attachment on the mandible. Ideally this was measured in medial view (figure S8), but could be estimated from the length of attachment of *m. adductor mandibulae superficialis* in lateral view. It was then divided by the total mandible length in order to correct for size.

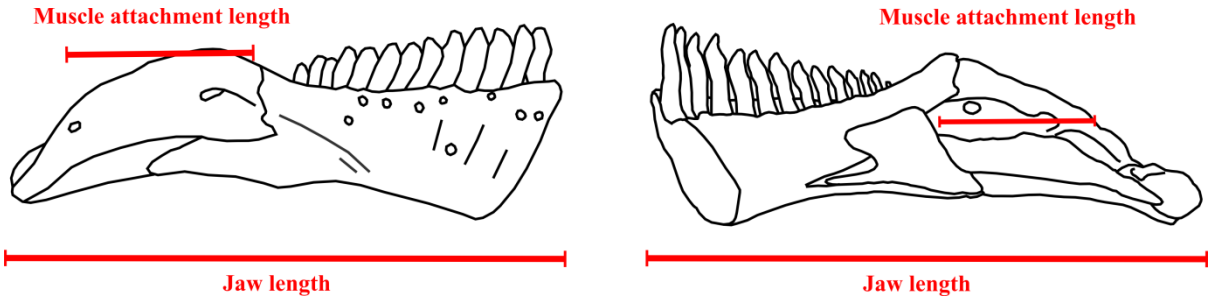

Figure S8: Illustration of the measurements taken for character C12, adductor fossa length/jaw length, demonstrated on both a lateral (left) and medial (right) view of the mandible of *C. lentus*. From Button *et al.* (2014).

(C13) Supratemporal fenestra length/skull length

The dimensions of the supratemporal fenestra were measured as a proxy for the attachment area of the temporal muscles (the *m. adductor externus* and *m. pseudotemporalis* groups) on the bones bordering the fenestra. Although the size of the subtemporal fenestra serves as the ultimate constraint on the size of the adductor chamber, this measurement was not taken as only a small number of sauropodomorph taxa have been adequately figured in ventral view.

The supratemporal fenestrae of sauropodomorphs are elliptical, but variable in shape (e.g. Upchurch *et al.*, 2004), necessitating measurements of both the anteroposterior and lateromedial axes to adequately express shape variance. For character C13 the anteroposterior length of the supratemporal fenestra was taken, and divided by the total length of the skull to correct for size (figure S9a).

This character was chosen over the dorsal measurement of supratemporal fenestra area used as it could be measured in specimens figured only in lateral view, thereby increasing taxon coverage.

(C14) Supratemporal fenestra breadth/skull width

For this character the lateromedial width of the supratemporal fenestra, perpendicular to the anteroposterior axis, was measured and divided by the width of the skull, as measured across the midpoint of the postorbital bar (figure S9b). This character was used in combination with character C13, rather than a single measurement of area, as it can be measured in taxa preserving only the skull roof, and can also be estimated from the posterior view where figures of the dorsal view are unavailable.

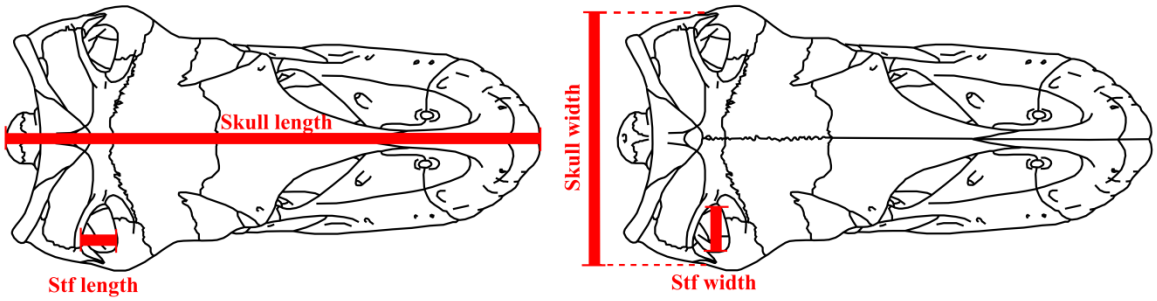

Figure S9: Illustration of the measurements taken for character C13, stf length/skull length (a) and character C14, stf breadth/skull breadth, illustrated on the skull of *C. lentus* in dorsal view. From Button *et al*. (2014).

(C15) Temporal muscle angle

The line of action of the temporal musculature varies markedly within Sauropodomorpha. In basal sauropodomorphs and 'broad-crowned' sauropods the line of action may lie at close to vertical, whereas in other forms like *Diplodocus* it is orientated at a low-angle from the skull long axis.

The vertical resultant force provided by the adductor musculature varies with the cosine of its angle from the vertical. As a result, muscles orientated closer to the vertical will be more efficient in terms of the proportion of input force translated to bite force, whereas those closer to the horizontal will be more effective at producing propalinal movements.

To measure this character a line was drawn between the midpoint of the temporal musculature origination area on the skull (the midpoint of the supratemporal fenestra) and the midpoint of the adductor muscle attachment along the dorsal margin of the surangular. The angle of this line to the vertical (perpendicular to the ventral margin of the skull) was then measured (figure S10).

In *Nigersaurus* the closed supratemporal fenestra, and the strong bend in the quadrate, render the position of the temporal musculature unclear (Sereno *et al*., 2007) and this measurement problematical (Button *et al*., 2014). This musculature was reconstructed as arising from the quadrate (after Sereno *et al*., 2007) (figure S10).

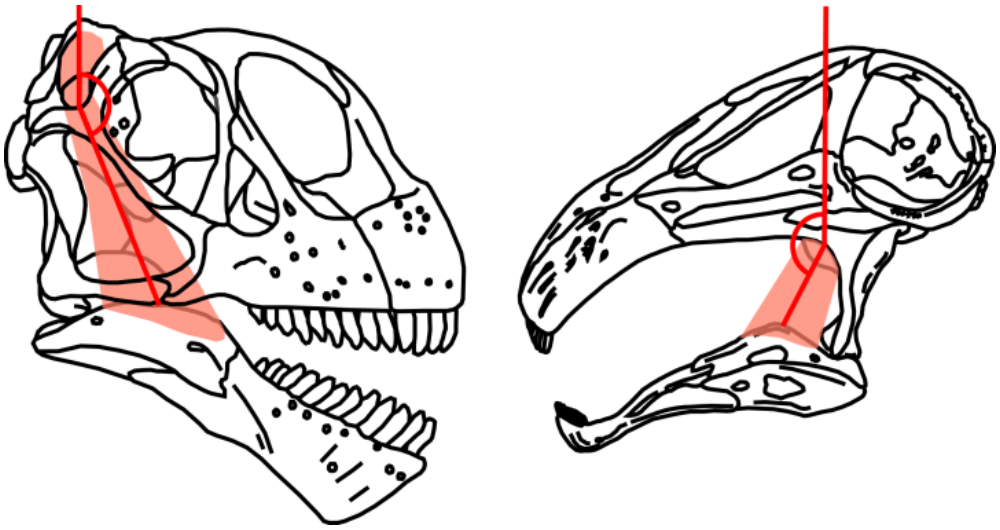

Figure S10: Illustration of the measurement taken for character C15, temporal muscle angle, from *C. lentus* (left) and *Nigersaurus* (right), in lateral view. From Button *et al*. (2014).

(C16) External mandibular fenestra area/mandible lateral area

The external mandibular fenestra is present in most archosaurs, where it increases the attachment area and accommodates the lateral bulging of the *m. adductor profundus* and *m. pseudotemporalis* muscles that attach within the mandibular fossa (Holliday, 2009). However, it also reduces the overall mass, and so robustness, of the mandible (Stubbs *et al*., 2013). Although large in many 'prosauropods', basal sauropods show a reduction in external mandibular fenestra size, and neosauropods close it altogether (Upchurch *et al*., 2004) (although this is then reversed in *Nigersaurus*: Sereno *et al*., 2007). To quantify external mandibular fenestra size the open area in lateral view was measured, and divided by the total lateral area of the mandible in order to account for size (figure S11).

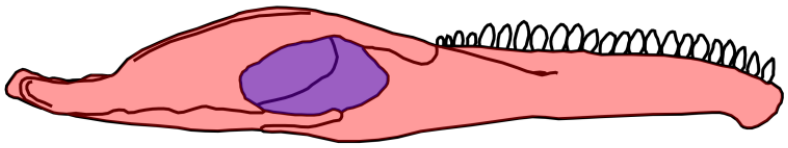

Figure S11: Illustration of the measurements taken for character C16, the relative area of the external mandibular fenestra, on the jaw of *P. engelhardti* in lateral view. Blue: the area of the external mandibular fenestra, in lateral view, which was divided by the total lateral area of the mandible (minus the teeth).

(C17) Retroarticular process length/mandible length

A longer retroarticular process results in a larger area of attachment for the *m. depressor mandibulae* musculature, which open the jaw. More rapid jaw opening may be important in faunivores, where multiple snapping bites may be important, but is of lesser importance in herbivores. Many 'prosauropod' taxa (e.g. *Jingshanosaurus*) possess elongate retroarticular processes. Additionally, a longer retroarticular process can accommodate an expanded articular glenoid, so this character can also serve as a proxy for propaliny potential for taxa in which the articular region is not preserved. Diplodocids show elongation of the retroarticular process associated with anteroposterior expansion of the articular. By contrast, most other sauropods

have very short retroarticular processes. For this character, the length of the retroarticular process (measured as the length of the jaw posterior to the articulation with the quadrate) was measured in lateral view, then divided by the total length of the jaw (figure S12).

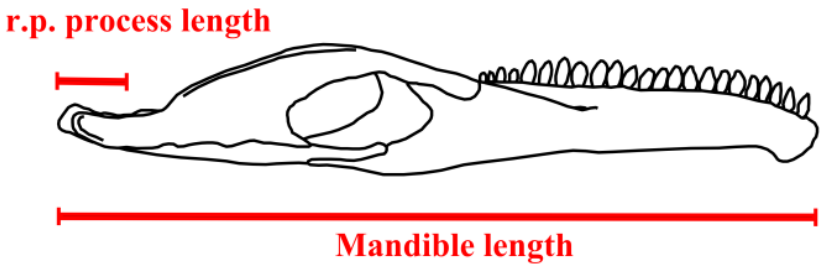

Figure S12: Illustration of the measurements taken for character C17, retroarticular process ("r.p. process") length/mandible length, shown on the mandible of *P. engelhardti*, in lateral view.

(C18) Premaxillary divergence angle (PMDA)

Snout shape is one of the most widely used proxies for diet in studies of both extant (e.g. Boue', 1970; Bell, 1971; Janis & Ehrhardt 1988; Gordon & Illius, 1989; Spencer, 1995) and extinct taxa (e.g. Solounias *et al*., 1988; Solounias & Moelleken, 1993; Dompierre & Churcher, 1996; Carrano *et al*., 1999), including studies on sauropods (Whitlock, 2011a). Although its success rate in distinguishing finer dietary categories is relatively low (Fraser & Theodor, 2011), it still serves as a reliable indicator between the two broad end-members of selective browsers and unselective grazers, which possess narrower and broader muzzles, respectively (Fraser & Theodor, 2011).

The PMDA is measured by drawing a line level with the midline tip of the snout, perpendicular to the long axis of the skull. The angle is then taken between this line and another drawn from the midline tip of the skull to the lateral edge of the premaxilla-maxilla suture, in dorsal view (figure S13).

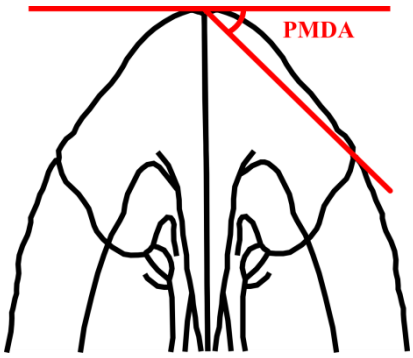

Figure S13: Illustration of the measurement of the character C18, the PMDA, on the snout of *C. lentus* in dorsal view. From Button *et al*. (2014).

A variety of metrics exist for the quantification of snout shape (see discussion in Whitlock, 2011a), but the PMDA was chosen as it can be measured from the premaxilla alone in the case of incomplete material, and calculated from anterior and lateral views if a dorsal view is absent. Additionally, in taxa from which only the mandible is known, the PMDA can be estimated from the position of the fourth dentary tooth (which would occlude with the final tooth of the premaxilla) relative to the anterior tip of the dentary.

(C19) Tooth angle

The orientation of the apical axes of the teeth varies considerably within Sauropodomorpha. Basal sauropodomorphs and some sauropods (e.g. *Nigersaurus*, Titanosauriformes) exhibit vertically orientated crowns (Barrett & Upchurch, 2007; Sereno *et al*., 2007), many other sauropods show moderate procumbency of the teeth (e.g. Upchurch *et al*., 2004), and most diplodocoids have highly procumbent dentitions (Barrett & Upchurch, 1994; Upchurch & Barrett, 2000). The orientation of the teeth influences cropping; vertically orientated teeth will be more efficient at force delivery and accommodation during static biting (Button *et al*., 2014). Procumbent dentitions are often observed in herbivores (Reisz & Sues, 2000), and would be more suitable for raking or plucking behaviors (Barrett & Upchurch, 1994; Upchurch & Barrett, 2000; Whitlock, 2011a; Young *et al*., 2012; Button *et al*., 2014).

Tooth angle was measured here as the angle between the apicobasal axes of the tooth crowns and a horizontal line drawn level with the maxillary/dentary alveolar margin (figure S14).

(C20) Tooth slenderness index

The ratio of tooth crown height to width, the slenderness index (SI) was developed as a phylogenetic character (Upchurch, 1998) but has since been used to classify sauropodomorphs into functional grades (Barrett & Upchurch 2005; Chure *et al*., 2010). The breadth of the crown will control the area available for shredding or processing plant matter at each tooth and shows a negative correlation with tooth replacement rate within Sauropoda (D'Emic *et al*., 2013). Also, in sauropods, more robust broad crowns are associated with taxa with greater bite forces and interdigitating occlusion, whereas narrow-crowns are typical of taxa exhibiting more precise nipping behaviors or lacking occlusion (Upchurch & Barrett, 2000). The slenderness index of each tooth was measured as the apicobasal height of each tooth crown, divided by its maximum breadth. This was performed across all preserved teeth from each specimen, with the mean value taken as the score for this character.

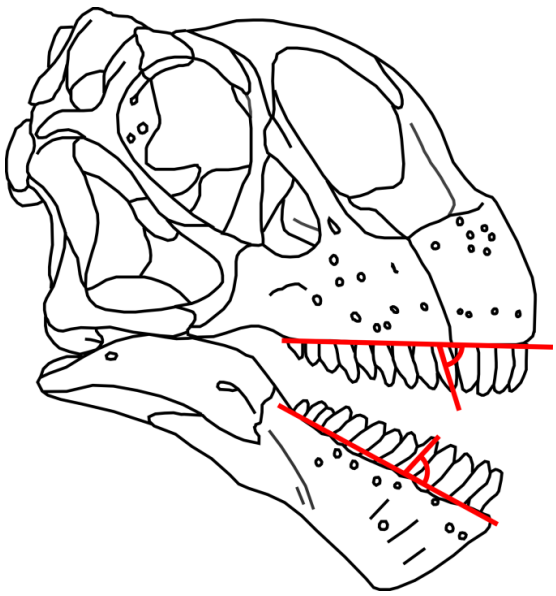

Figure S14: Illustration of the measurements taken for character C19, tooth angle, on the skull and jaws of *C. lentus* in lateral view. From Button *et al*. (2014).

Binary characters

(C21) Heterodont dentition: absent (0)/present (1)

Sauropod dentitions are homodont, although tooth size decreases posteriorly (Upchurch *et al*., 2004). Most basal sauropodomorphs, in contrast, exhibit moderate heterodonty, where the premaxillary and often the anterior dentary teeth (Galton & Upchurch, 2004) and occasionally the anteriormost maxillary teeth (Prieto-Márquez & Norell, 2011) are conical, whereas the remaining maxillary and dentary teeth are smaller and lanceolate (Galton & Upchurch, 2004; figure). Heterodonty increases dental complexity and reflects the number and disparity of roles the dentition is required to perform. Whereas the entire toothrow in sauropods was utilized for cropping (Christiansen, 1999; Upchurch & Barrett, 2000), in basal taxa the larger anterior dentition would have been used for plucking and the posterior teeth for pulping/shredding (Barrett & Upchurch, 2007).

Heterodonty was scored simply as present or absent in all taxa, on the basis of whether or not they showed distinctive variance between the anteriormost teeth and the remainder of the dentition.

(C22) Denticulate dentition: absent (0)/present (1)

The teeth of extant herbivorous iguanines bear coarse denticles, arranged obliquely to the long axis of the crown (Throckmorton, 1976; Barrett, 2000), which assist in tearing plant matter (Throckmorton, 1976). Similarly denticulate teeth are often taken as a general correlate of herbivory in fossil taxa (Reisz & Sues, 2000; Sues 2000).

Almost all basal sauropodomorphs, and the majority of non-neosauropod sauropods, bear similar coarse, oblique denticles on the mesiodistal tooth margins (Galton, 1984, 1985a, b; Barrett, 2000; Upchurch & Barrett, 2000; Galton & Upchurch, 2004; Upchurch *et al*., 2004;

Barrett & Upchurch, 2007; figure 5.6a-c), although in older, worn, teeth they will be replaced by wear facets (e.g. Allain & Aquesbi, 2008; He *et al*., 1988: fig. 17).

Turiasaurians (Royo-Torres & Upchurch, 2012) lack denticles. In neosauropods denticles are generally absent (Upchurch & Barrett, 2000; Galton & Upchurch, 2004; figure 5.6d-f), apart from *Brachiosaurus* and *Giraffatitan*, which occasionally show the incipient development of small, apically restricted denticles (Janensch, 1935-6; Carpenter & Tidwell, 1998; Upchurch & Barrett, 2000; Galton & Upchurch, 2004), and small denticles may be present in rare cases in *Camarasaurus* (Upchurch & Barrett, 2000). Similarly, the titanosaur *Tapuiasaurus* demonstrates the incipient development of crenulations along the tooth carinae (Zaher *et al*., 2011). However, as in the latter cases denticles are rarely developed, small and quickly replaced by apical wear facets following use, they were considered functionally absent for the purposes of this study.

(C23) Recurved teeth: absent (0)/present (1)

Recurved teeth are associated with carnivory, where their shape helps to prevent the escape of pierced prey items (Reisz & Sues 2000). The basalmost sauropodomorphs, such as *Eoraptor* (Sereno *et al*., 1993, 2013), and some more derived 'prosauropods', such as *Jingshanosaurus* (Zhang & Yang, 1994: fig. 9), possess recurved teeth in the dentition, whereas most sauropodomorphs lack widespread tooth recurvature.

(C24) Overlapping tooth crowns: absent (0)/present (1)

The majority of basal sauropodomorphs (Galton & Upchurch, 2004) and 'broad-crowned' sauropods (Upchurch *et al*., 2004) demonstrate *en echelon* tooth arrangement of the maxillary and dentary teeth; with overlap between the mesiodistally expanded tooth crowns. This arrangement results in a more continuous cutting surface across the length of the toothrow for

shredding plant matter. Tooth overlap was scored as present or absent on the basis of whether the majority of maxillary and dentary teeth demonstrate an imbricate arrangement or not.

(C25) Tooth-tooth wear facets: absent (0)/present (1)

Although lost in some lineages (such as Diplodocoidae: Barrett & Upchurch, 1994; Upchurch & Barrett, 2000; Young *et al*., 2012) the presence of well-developed wear facets, resulting from shearing, static occlusion, is a synapomorphy of Sauropoda (Barrett & Upchurch, 2007). Tooth-tooth wear facets are absent in all more basal sauropodomorphs (Barrett & Upchurch, 2007), which instead would have limited to orthal pulping of fodder, via puncture-crushing by individual tooth crowns. A possible exception to this is *Adeopapposaurus*, where complimentary facets occur on the third and fourth premaxillary teeth and the opposing first and second dentary teeth (Martínez, 2009). However, wear facets are absent in the rest of the dentition (Martínez, 2009), so a shearing bite functionally analogous to that of most sauropods was not present. As a result, occlusion was scored as "absent" in *Adeopapposaurus*. This character was included in addition to the following characters detailing occlusal pattern as it was considered that two taxa sharing tooth-tooth occlusion, even if demonstrating different occlusal styles, would be more functionally similar than another taxon which lacked tooth-tooth occlusion entirely.

(C26) Interdigitating tooth occlusion: absent (0)/present (1)

'Broad-crowned' sauropods all demonstrate the development of mesiodistal wear facets on the apical "shoulders" of the teeth, as a result of each tooth occluding between the apices of two others on the opposite jaw (Upchurch & Barrett, 2000; Upchurch *et al*., 2004; Barrett & Upchurch, 2005).

(C27) Precise tooth occlusion: absent (0)/present (1)

Brachiosaurids (Calvo, 1994; Upchurch & Barrett, 2000; Barrett & Upchurch, 2005), titanosaurs (Calvo, 1994; Upchurch & Barrett, 2000; Barrett & Upchurch, 2005), dicraeosaurids (at least in *Dicraeosaurus* [Janensch, 1935-6; Upchurch, 1999; Chrisitansen, 2000; Upchurch & Barrett, 2000; Barrett & Upchurch, 2005] and cf. *Amargasaurus* [Apesteguía, 2007]) and rebbachisaurids (at least in *Nigersaurus* [Sereno & Wilson, 2005; Sereno *et al*., 2007; figure 5.6e] and *Limaysaurus* [Salgado *et al*., 2004]) show apical wear facets, as a result of each tooth contacting a single other tooth on the opposing jaw (Calvo, 1994; Upchurch & Barrett, 2000; Barrett & Upchurch, 2005; *contra* Christiansen, 2000).

Giraffatitan (Calvo, 1994; Upchurch & Barrett, 2000) *Dicraeosaurus* (Christiansen, 2000), *Nemegtosaurus* (Wilson, 2005), *Tapuiasaurus* (Zaher *et al*., 2011) and some other titanosaurs (García & Cerda, 2010) show the rare development of v-shaped mesiodistal wear facets. However, given their scarcity relative to apical facets, 'precision-shear' is taken as the dominant occlusion pattern in these cases, with mesiodistal wear the product either of mismatch resulting from dental aberrations (García & Cerda, 2010), or being formed only late in tooth ontogeny (Wilson, 2005; Zaher *et al*., 2011; Button *et al*., 2014). Similarly, the presence of both labial and lingual facets in diplodocoid teeth (Barrett & Upchurch, 1994; Upchurch & Barrett, 2000; Christiansen, 2000; Sereno & Wilson, 2005) and some titanosaurs (García & Cerda, 2010) is taken as a result of either tooth-food wear (Barrett & Upchurch, 1994; Upchurch & Barrett, 2000; Christiansen, 2000; Sereno & Wilson, 2005) or as a result of dental mismatch during the tooth replacement cycle (García & Cerda, 2010).

(C28) Lateral plates: absent (0)/present (1)

The 'lateral plates' are marginal extensions of the tooth-bearing bones that cover the basal third of the tooth crowns labially (Upchurch, 1998) and are thought to have braced the teeth against laterally-oriented forces during cropping (Barrett & Upchurch, 1994; Upchurch & Barrett,

2000). *Aardonyx* (Yates *et al*., 2010) and more derived taxa possess premaxillary, maxillary and dentary lateral plates. The distribution of this character is slightly problematical; *Aardoynx* possesses premaxillary, maxillary and dentary lateral plates (Yates *et al*., 2010), whereas lateral plates are entirely absent in *Melanorosaurus* (Yates, 2007). *Chinshakiangosaurus* (Upchurch *et al*., 2007) and *"Kunmingosaurus"* (Barrett & Upchurch, 2007) each possess dentary lateral plates, suggesting that they appeared first (Barrett & Upchurch, 2007). However, the absence of other cranial material in the latter two taxa makes this difficult to assess, and separate characters for the occurrence of lower and upper lateral plates would differ only by two unknown entries for the scoring of the maxillary lateral plates in both taxa. As a result, only a single lateral plate character was included, with plates scored as present in those taxa showing any indication of them along either the lower or upper toothrow.

(C29) Self-supporting tooth battery: absent (0)/present (1)

Nigersaurus shows the development of a sophisticated dental battery, featuring extremely high tooth replacement rates and increased tooth numbers, housed in an anteroposteriorly short but laterally expanded toothrow (Sereno & Wilson, 2005; Sereno *et al*., 2007). Wear facets cross multiple teeth, which would have erupted and functioned as a single broad blade during cropping (Sereno & Wilson, 2005; Sereno *et al*., 2007). This morphological complex was deemed sufficiently functionally derived to be scored for an independent category here. The general paucity of rebbachisaurid cranial remains makes the distribution of this character difficult to assess; its absence in *Demandasaurus* (Fernández-Baldor *et al*., 2011), a closely related nigersaurine (Fanti *et al*., 2013), suggests that it was unique to *Nigersaurus*. Nevertheless, this character was scored as "?" in the rebbachisaurid *Limaysaurus* due to the absence of comparable material from Limaysaurinae.

S3. Multivariate analysis

Taxon scores for the continuous metrics were *z*-transformed. This corrects for differences in size and variability by scaling each measurement to have a mean value of 0 and standard deviation of 1. The transformed data were then subjected to principle coordinate analysis (PCO), conducted in PAST (Hammer *et al*., 2001), utilizing the Gower dissimilarity index (Gower, 1971). Gower dissimilarity was chosen as it can be applied to mixed datasets containing both continuous and categorical data. The Mardia (1978) correction was applied to negative eigenvalues.

The first two axes strongly capture the functional variation present within the clade, accounting for >50% of the observed variance. After this variance scores quickly tail off to <1% in PC axes 12 and above. The strength of character loading on each axis was tested through linear correlations and calculation of the Spearman's Rank Correlation Coefficient, performed in PAST. Results are given in table S3.

The plot of PC axes 1 & 2 is shown in more detail in figure S15, with all the positions of all taxa labelled. Variance along PC axis 3 is illustrated in figure S16. The taxonomic content of each of the sauropodomorph groups using during plotting is given in Table S4.

	r values and r^2 values		*p*- values	
	PC1	**PC2**	**PC1**	**PC2**
C1 – Gape length	-0.475 *0.225*	0.478 *0.228*	**2.607E-07**	**1.879E-04**
C2 – Anterior MA	-0.295 *0.087*	0.460 *0.2116*	**0.022**	**1.6648E-06**
C3 – Posterior MA	0.057 *3.301E-03*	0.582 *0.339*	0.838	**2.237E-09**
C4 – Articular offset	-5.671E-03 *3.216E-05*	0.270 *0.073*	0.609	**6.973E-03**
C5 – Quadrate:articular	0.351 *0.123*	0.233 *0.054*	**9.033E-04**	0.299
C6 – Max jaw depth:length	-0.486 *0.236*	0.237 *0.056*	**9.228E-07**	**4.921E-03**
C7 – Average jaw depth:length	-0.507 *0.257*	0.430 *0.185*	**8.995E-09**	**5.344E-05**
C8 – Toothrow:skull length	0.558 *0.311*	0.219 *0.048*	**2.464E-11**	0.323
C9 – Toothrow:jaw length	0.460 *0.211*	0.426 *0.181*	**7.371E-04**	**1.164E-04**
C10 – Symphysis:jaw length	-0.428 0.184	0.487 *0.237*	**1.533E-08**	**4.779E-04**
C11 – Symphysis:jaw angle	-0.382 *0.146*	0.124 *0.015*	**4.523E-05**	0.145
C12 – Adductor fossa:jaw length	0.186 *0.035*	0.275 *0.076*	0.143	**0.016**
C13 – Stf length:skull length	0.608 *0.370*	-0.071 *5.044E-03*	**1.358E-14**	0.901
C14 – Stf breadth:skull breadth	0.328 *0.107*	0.320 *0.103*	**7.548E-03**	**3.534E-04**
C15 – Muscle angle	0.413 *0.171*	0.135 *0.018*	**2.607E-07**	0.436
C16 – e.m.f.:jaw area	0.543 *0.295*	-0.279 0.0780	**1.33E-14**	**0.026**
C17 – Retroarticular process length:jaw length	0.155	-0.378	**0.041**	**3.551E-03**

	0.024	0.143		
C18 – PMDA	0.674 *0.455*	0.341 *0.116*	**6.739E-15**	**0.029**
C19 – Tooth angle	0.366 *0.134*	0.017 *2.728E-04*	**5.254E-03**	0.561
C20 – SI	-0.750 *0.562*	-0.411 *0.169*	**3.366E-11**	**0.016**
C21 – Heterodont dentition	0.835 *0.697*	-0.190 *0.036*	**4.989E-16**	0.358
C22 – Tooth denticles	0.856 *0.733*	0.153 *0.024*	**2.665E-18**	0.228
C23 – Recurved teeth	0.343 *0.118*	-0.273 *0.075*	**1.638E-03**	**0.017**
C24 – Overlapping teeth	0.750 *0.563*	0.405 *0.164*	**3.364E-12**	**1.284E-03**
C25 – Occlusion	-0.690 *0.476*	0.630 *0.396*	**2.434E-11**	**9.479E-08**
C26 – Interdigitating occlusion	-0.029 *8.275E-04*	0.844 *0.712*	0.912	**2.908E-11**
C27 – Precise occlusion	-0.737 0.543	-0.123 *0.015*	**1.138E-12**	0.612
C28 – Lateral plate	-0.824 *0.679*	0.336 *0.113*	**3.993E-17**	**0.017**
C29 – Dental battery	-0.172 *0.030*	-0.129 *0.017*	0.149	0.217

Table S3: Character loadings on the first two PC axes. Quoted r and r^2 values are from linear regressions of scores for each character against PC axes scores, *p*-values are from Spearman's rank correlation of character scores with PC axis scores.

	Group	Definition	Taxa
"Prosauropoda"	"Basalmost Sauropodomorphs"	Non-plateosaurian sauropodomorphs.	*Panphagia protos*, *Eoraptor lunensis*, *Pampadromaeus barberenai*, *Pantydraco caducus*, *Arcusaurus pereirabdolorum*, *Thecodontosaurus antiquus*, *Efraasia minor*
	"Basal Plateosaurians"	Non-sauropodiform plateosaurians.	*Unaysaurus tolentinoi*, *Plateosaurus engelhardti*, *P. erlenbergiensis*, *Riojasaurus incertus*, *Sarahsaurus aurifontanalis*, *Massospondylus carinatus*, *M. kaalae*, *Adeopapposaurus mognai*, *Leyesaurus marayensis*, *Lufengosaurus huenei*, *Coloradisaurus brevis*
	"Basal Sauropodiformes"	Non-sauropod sauropodiforms.	*Jingshanosaurus xinwaensis*, *Yunnanosaurus huangi*, *Chuxiongosaurus lufengensis*, *Anchisaurus polyzelus*, *Mussaurus patagonicus*, *Aardonyx celestae*, *Melanorosaurus readi*, *"Kunmingosaurus" wudingensis*, *Lamplughsaura dharamensis*, *Chinshakiangosaurus chunghoensis*
"Basal Sauropoda"		Non-diplodocoid and non-titanosauriform sauropods.	*Tazoudasaurus naimi*, *Shunosaurus lii*, *Patagosaurus fariasi*, *Mamenchisaurus youngi*, *M. jingyanensis*, *M. sinocanadorum*, *Omeisaurus tianfuensis*, *Omeisaurus maoianus*, *Turiasaurus riodevensis*, *Jobaria tiguidensis*, *Atlasaurus imelakei*, *Camarasaurus lentus*, *Camarasaurus grandis*
Diplodocoidea	Rebbachisauridae	The most inclusive clade including *Rebbachisaurus garasbae* but not *Diplodocus longus* (Whitlock 2011).	*Demandasaurus darwini*, *Nigersaurus taqueti*, *Limaysaurus tessonei*
	Dicraeosauridae	The most inclusive clade including *Dicraeosaurus hansemanni* and not *Diplodocus longus* (Whitlock 2011).	*Suuwassea emilieae*, *Dicraeosaurus hansemanni*, *Amargasaurus cazaui*
	Diplodocidae	The most inclusive clade including *Diplodocus longus* but not *Dicraeosaurus hansemanni* (Whitlock 2011).	*Apatosaurus louisae*, *Kaatedocus sineri*, *Tornieria africana*, *Diplodocus carnegii*, *D. longus*
Brachiosauridae		The most inclusive clade including *Brachiosaurus altithorax* but not *Saltasaurus loricatus* (Wilson & Sereno 1998).	*Europasaurus holgeri*, *Brachiosaurus sp.*, *Abydosaurus mcintoshi*, *Giraffatitan brancai*
Euhelopodidae		Neosauropods more closely related to *Euhelopus zdanskyi* than *Neuquensaurus australis* (D'Emic 2012).	*Euhelopus zdanskyi*
Titanosauria		The least inclusive clade including *Andesaurus delgadoi* and *Saltasaurus loricatus* (Mannion *et al.* 2013).	*Malawisaurus dixeyi*, *Karongasaurus gittelmani*, *Ampelosaurus atacis*, *Antarctosaurus wichmannianus*, *Brasilotitan nemophagus*, *Bonitasaura salgadoi*, *Quaesitosaurus orientalis*, *Nemegtosaurus mongoliensis*, *Tapuiasaurus macedoi*, *Rapetosaurus krausei*

Table S4: The groups by which taxa were plotted in the biomechanical morphospace plots.

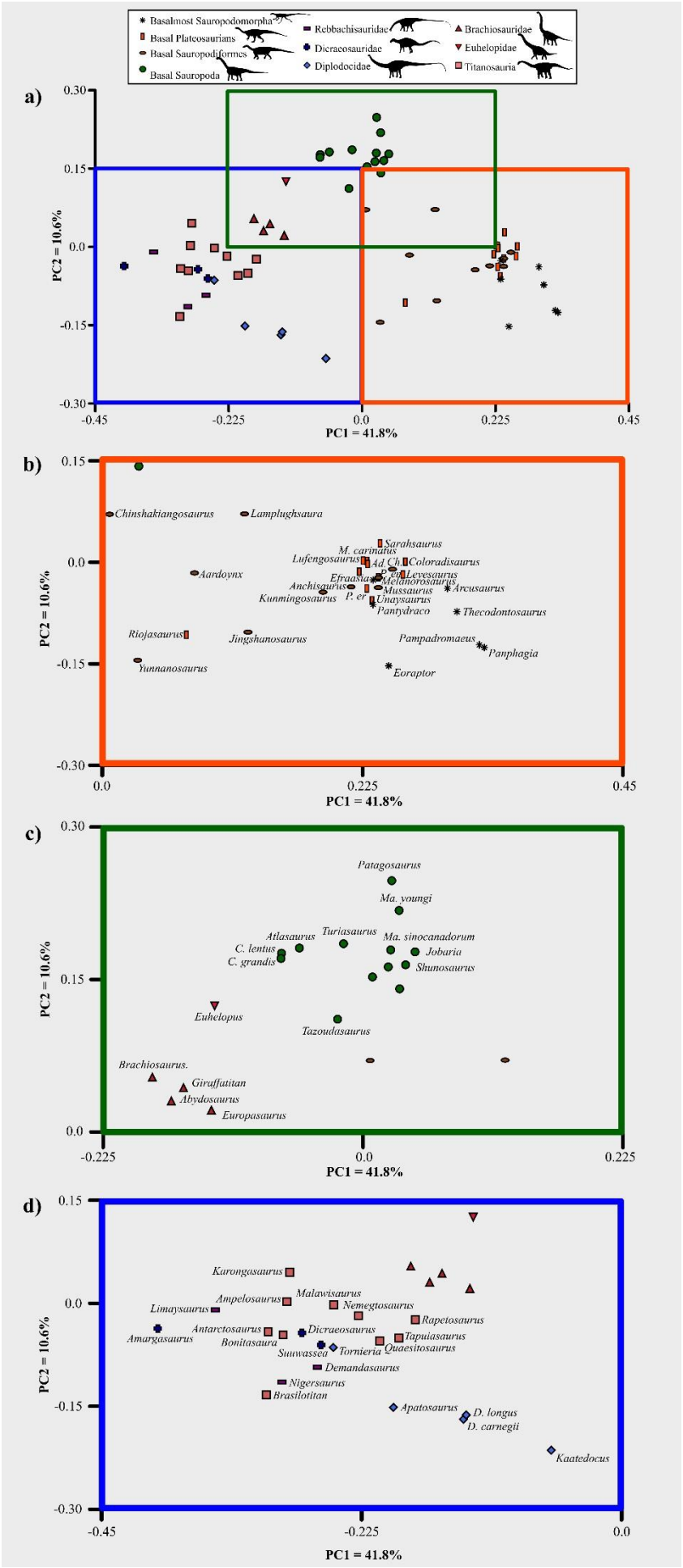
Basalmost Sauropodomorpha
Basal Plateosaurians
Basal Sauropodiformes
Basal Sauropoda
Rebbachisauridae
Dicraeosauridae
Diplodocidae
Brachiosauridae
Euhelopidae
Titanosauria
a)
PC2 = 10.6%
PC1 = 41.8%
b)
Chinshakiangosaurus
Lamplughsaura
Sarahsaurus
M. carinatus
Lufengosaurus
Ad. Ch.
Coloradisaurus
Aardoynx
Efraasia
Levesaurus
Melanorosaurus
Anchisaurus
Mussaurus
Arcusaurus
Kunmingosaurus
P. er
Unaysaurus
Pantydraco
Thecodontosaurus
Riojasaurus
Jingshanosaurus
Pampadromaeus
Panphagia
Yunnanosaurus
Eoraptor
c)
Patagosaurus
Ma. youngi
Atlasaurus
Turiasaurus
Ma. sinocanadorum
C. lentus
C. grandis
Jobaria
Shunosaurus
Euhelopus
Tazoudasaurus
Brachiosaurus.
Giraffatitan
Abydosaurus
Europasaurus
d)
Karongasaurus
Malawisaurus
Ampelosaurus
Nemegtosaurus
Limaysaurus
Rapetosaurus
Antarctosaurus
Dicraeosaurus
Amargasaurus
Bonitasaura
Tapuiasaurus
Suuwassea
Tornieria
Quaesitosaurus
Demandasaurus
Nigersaurus
Brasilotitan
Apatosaurus
D. longus
D. carnegii
Kaatedocus

Figure S15: Breakdowns of the first two PC axes of the biomechanical morphospace, with the positions of all taxa labelled. Abbreviated genus names as follows: *P.* = *Plateosaurus*, *Ad.* = *Adeopapposaurus*, *Ma.* = *Massospondylus*, *Ch.* = *Chuxiongosaurus*, *Ma.* = *Mamenchisaurus*, *O.* = *Omeisaurus*, *C.* = *Camarasaurus*, *D.* = *Diplodocus*. a) Full plot of PC axes one and two, with the regions focussed upon in b-d) indicated. b) Distribution of 'prosauropod taxa. c) Distribution of 'broad-crowned' sauropods and Brachiosaurids. d) Distribution of 'narrow-crowned' taxa.

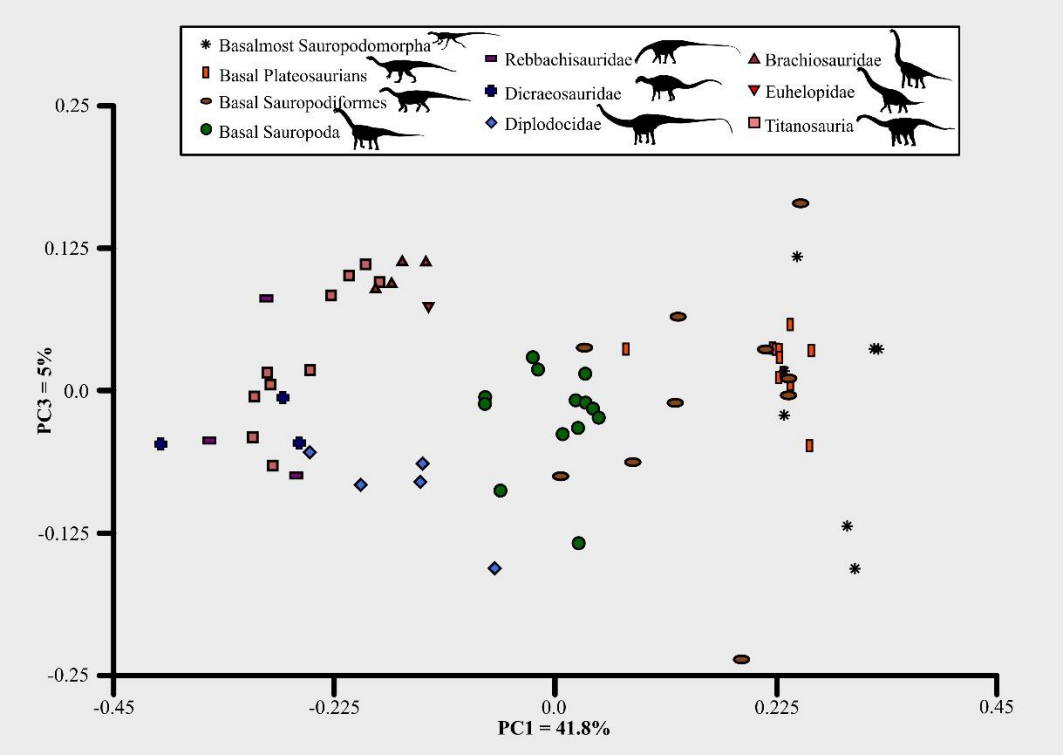

Figure S16: Biomechanical morphospace plot of PC axes one versus three.

S4. Disparity analysis additional results

Sauropods and 'prosauropods' exhibit similar overall levels of craniodental functional disparity, regardless of the metric used (figure S17a-d). Comparison of the three main craniodental functional grades demonstrates that 'broad-crowned' sauropods exhibit lower disparity than either 'narrow-crowned' or 'prosauropod' taxa (figure S17e-h). However, 'prosauropods' only demonstrate significantly greater levels of disparity than 'broad-crowned' taxa under variance-based metrics (figure S17e-f). The taxonomic content of these three functional grades is given in Table S5.

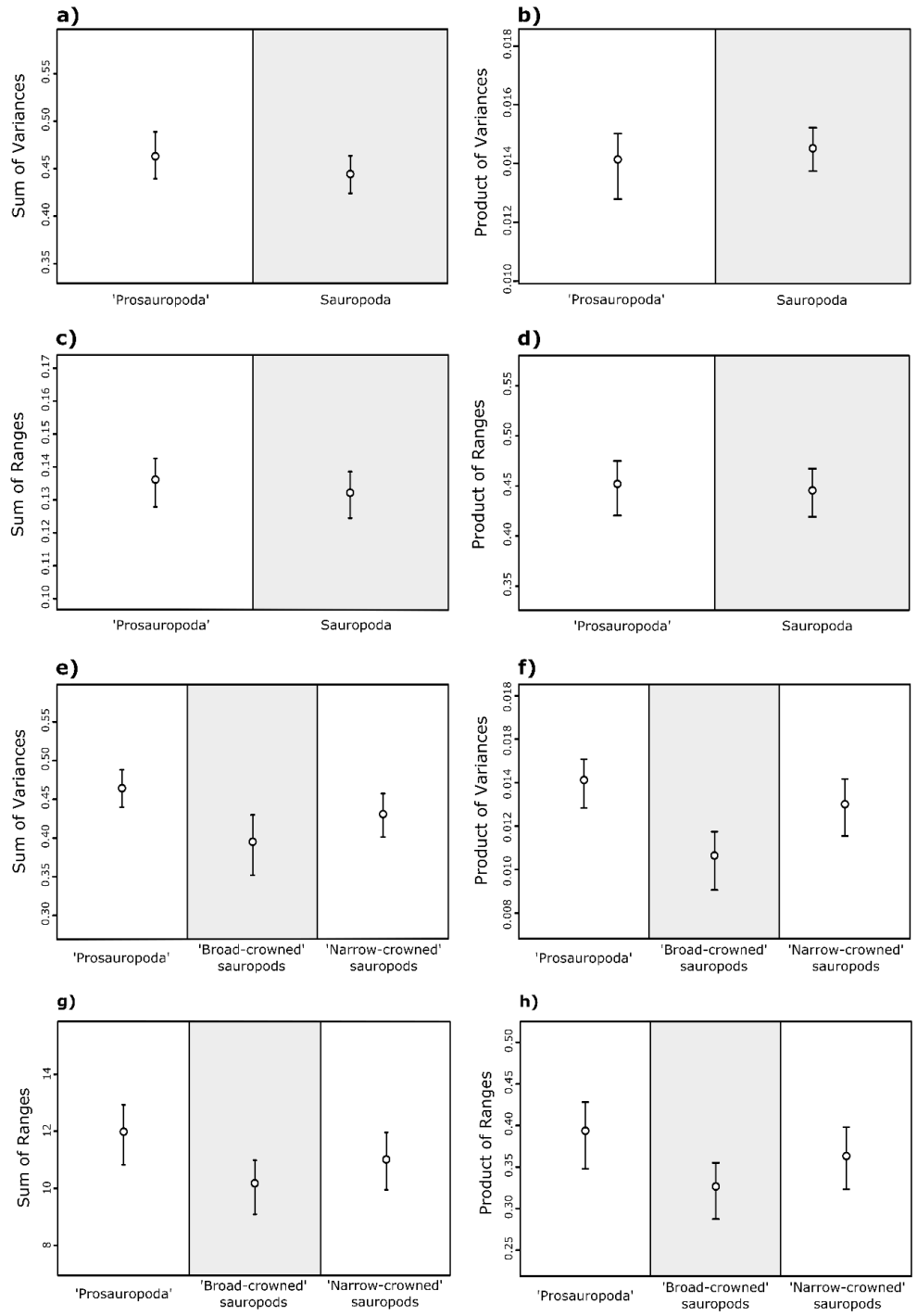

Figure S17: Comparisons of craniodental functional disparity calculated from scores on the first 29 PC axes for a-d) "prosauropods" vs. sauropods and e-h) the three functional grades ("prosauropod", "broad-crowned" sauropods [including *Euhelopus*] and "narrow-crowned" sauropods). Brachiosaurids were omitted from the analysis comparing the three functional grades. 95% confidence intervals calculated from bootstrapping with 1000 replicates given. The following metrics are reported: a, e) Sum of Variances, b, f) Product of Variances, c, g) Sum of Ranges, d, h) Product of Ranges.

Functional grade	Description	Taxa
"Prosauropoda"	Non-sauropod sauropodomorphs	*Panphagia protos*, *Eoraptor lunensis*, *Pampadromaeus barberenai*, *Pantydraco caducus*, *Arcusaurus pereirabdolorum*, *Thecodontosaurus antiquus*, *Efraasia minor*, *Unaysaurus tolentinoi*, *Plateosaurus engelhardti*, *P. erlenbergiensis*, *Riojasaurus incertus*, *Sarahsaurus aurifontanalis*, *Massospondylus carinatus*, *M. kaalae*, *Adeopapposaurus mognai*, *Leyesaurus marayensis*, *Lufengosaurus huenei*, *Coloradisaurus brevis*, *Jingshanosaurus xinwaensis*, *Yunnanosaurus huangi*, *Chuxiongosaurus lufengensis*, *Anchisaurus polyzelus*, *Mussaurus patagonicus*, *Aardonyx celestae*, *Melanorosaurus readi*, "*Kunmingosaurus*" *wudingensis*, *Lamplughsaura dharamarensis*, *Chinshakiangosaurus chunghoensis*
"Broad-crowned sauropods"	Non-neosauropod sauropods, *Camarasaurus*, Euhelopodidae	*Tazoudasaurus naimi*, *Shunosaurus lii*, *Patagosaurus fariasi*, *Mamenchisaurus youngi*, *M. jingyanensis. M. sinocanadorum*, *Omeisaurus tianfuensis*, *O. maoianus*, *Turiasaurus riodevensis*, *Jobaria tiguidensis*, *Atlasaurus imelakei*, *Camarasaurus lentus*, *Camarasaurus grandis*, *Euhelopus zdanyski*
"Narrow-crowned sauropods"	Diplodocoidea, lithostrotian titanosaurs	*Demandasaurus darwini*, *Nigersaurus taqueti*, *Limaysaurus tessonei*, *Suuwassea emilieae*, *Dicraeosaurus hansemanni*, *Amargasaurus cazaui*, *Apatosaurus louisae*, *Kaatedocus siberi*, *Tornieria africana*, *Diplodocus carnegii*, *D. longus*, *Malawisaurus dixeyi*, *Karongasaurus gittelmani*, *Ampelosaurus atacis*, *Antarctosaurus wichmannianus*, *Brasilotitan nemophagus*, *Bonitasaura salgadoi*, *Quaesitosaurus orientalis*, *Nemegtosaurus mongoliensis*, *Tapuiasaurus macedoi*, *Rapetosaurus krausei*

Table S5. The taxonomic content of the three primary craniodental morphological and functional grades observed within Sauropodomorpha.

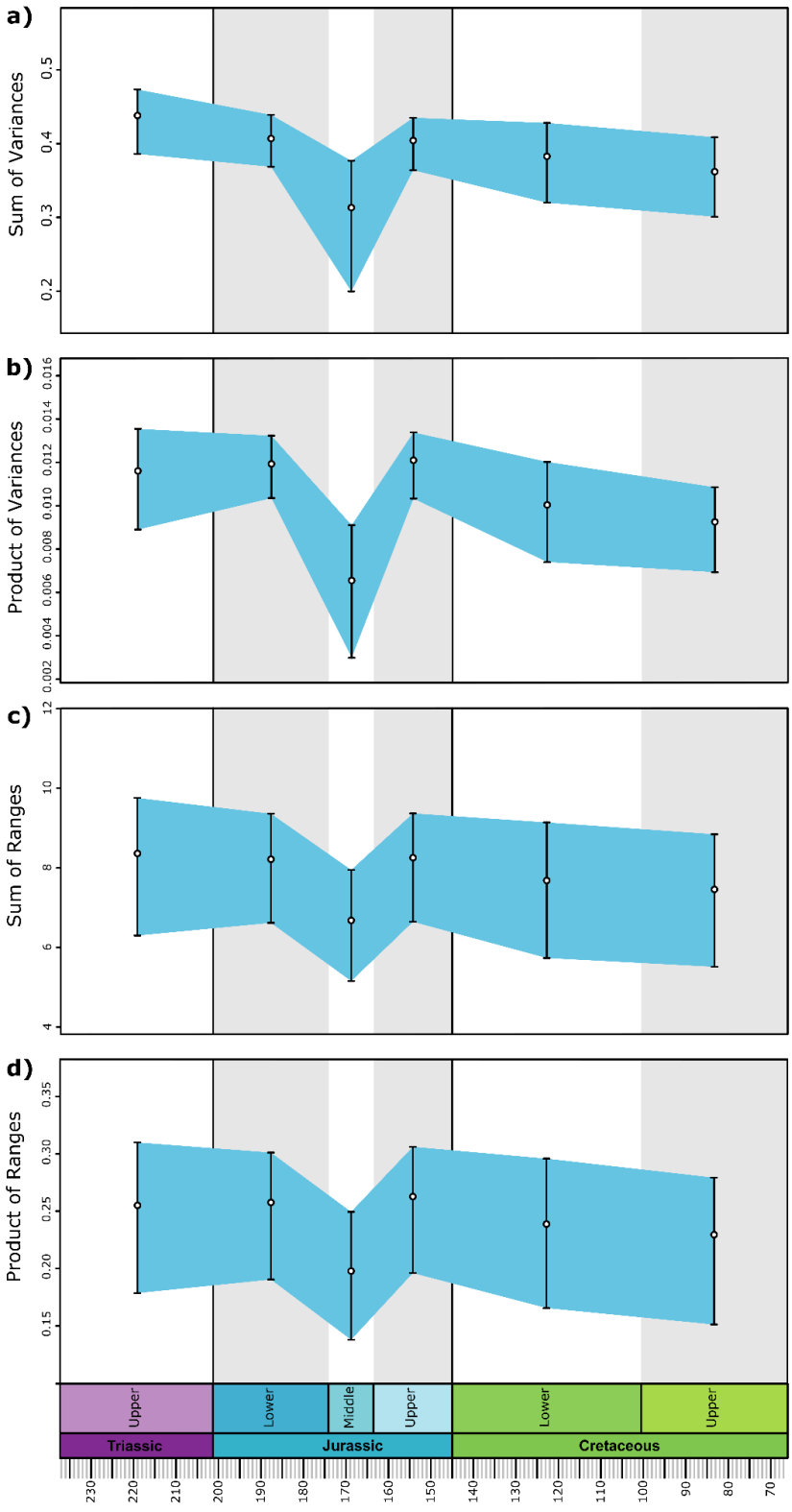

Figure S18: Sauropodomorph craniodental functional disparity through time, as calculated from scores on the first 29 PC axes. Bars refer to 95% confidence intervals, calculated from bootstrapping with 1000 replicates. The following metrics are reported: a) Sum of Variances, b) Product of Variances, c) Sum of Ranges, d) Product of ranges.

Patterns of total craniodental functional disparity through time are also broadly robust to the disparity metric used (figure S18). No significant differences between time bins are observed with the exception of the Middle Jurassic, which shows significantly lower disparity than the Early Jurassic and Late Jurassic under product of variances (figure S18b). However, this result is observed under product of variances only; no significant differences between time bins are observed for other disparity metrics (figure S18).

S5. Phylogeny

A single taxon–character matrix including the majority of sauropodomorph taxa does not exist. Instead, an informal supertree of the 117 taxa represented by PC axis and/or body mass data (figures S19, S20) was constructed based upon published topologies: primarily after Benson *et al*. (2014), with additional input from other sources for basal sauropodomorphs (Apaldetti *et al*., 2011, 2013, 2014; Otero & Pol, 2013; McPhee *et al*., 2014), basal sauropods (Allain & Aquesbi, 2008; Wilson & Upchurch, 2009; Royo-Torres & Upchurch 2012), Diplodocoidea (Whitlock, 2011b; Fanti *et al*., 2013), and Macronaria (Gallina & Apesteguía, 2011; Zaher *et al*., 2011; D'Emic, 2012; Mannion *et al*., 2013; Gorscak *et al*., 2014; Lacovara *et al*., 2014), with the position of *Brasilotitan nemophagus* based upon the comparisons of Machado *et al*. (2013).

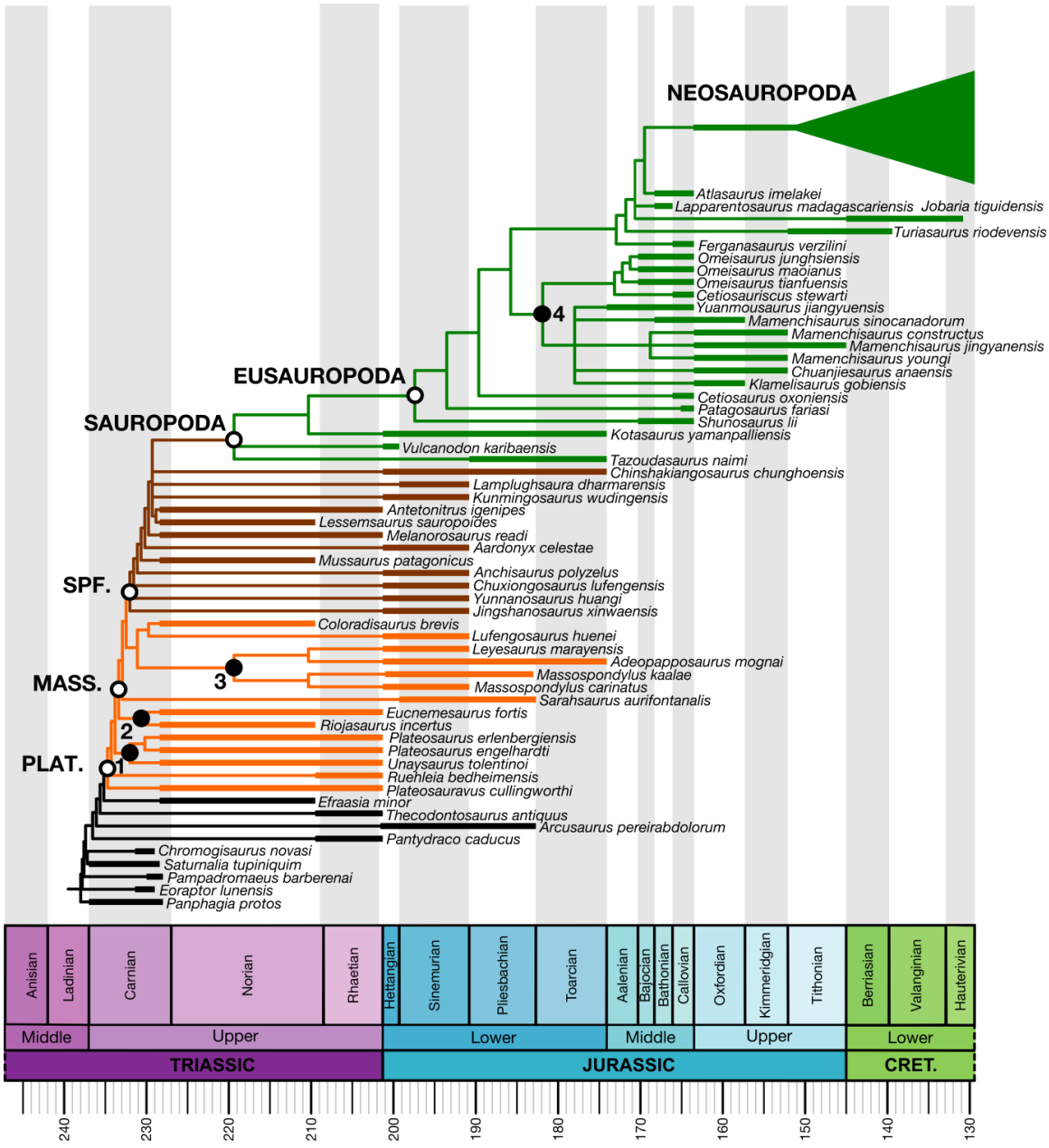

561

562 Figure S19: Informal supertree of the Sauropodomorpha, as used in this study, based primarily on Benson *et al.*
563 (2014). Neosauropod interrelationships are given in figure 5.8. Taxa are colored as in the biomechanical
564 morphospace plots (figures 2-5). Higher-order clades are labelled, abbreviations as follows: PLAT. – Plateosauria;
565 MASS. – Massopoda; SPF. – Sauropodiformes. Numbered nodes refer to the following families: 1-
566 Plateosauridae, 2- Riojasauridae, 3- Massospondylidae, 4- Mamenchisauridae. Tree plotted using the Strap
567 package (Bell & Lloyd, 2015) in R.

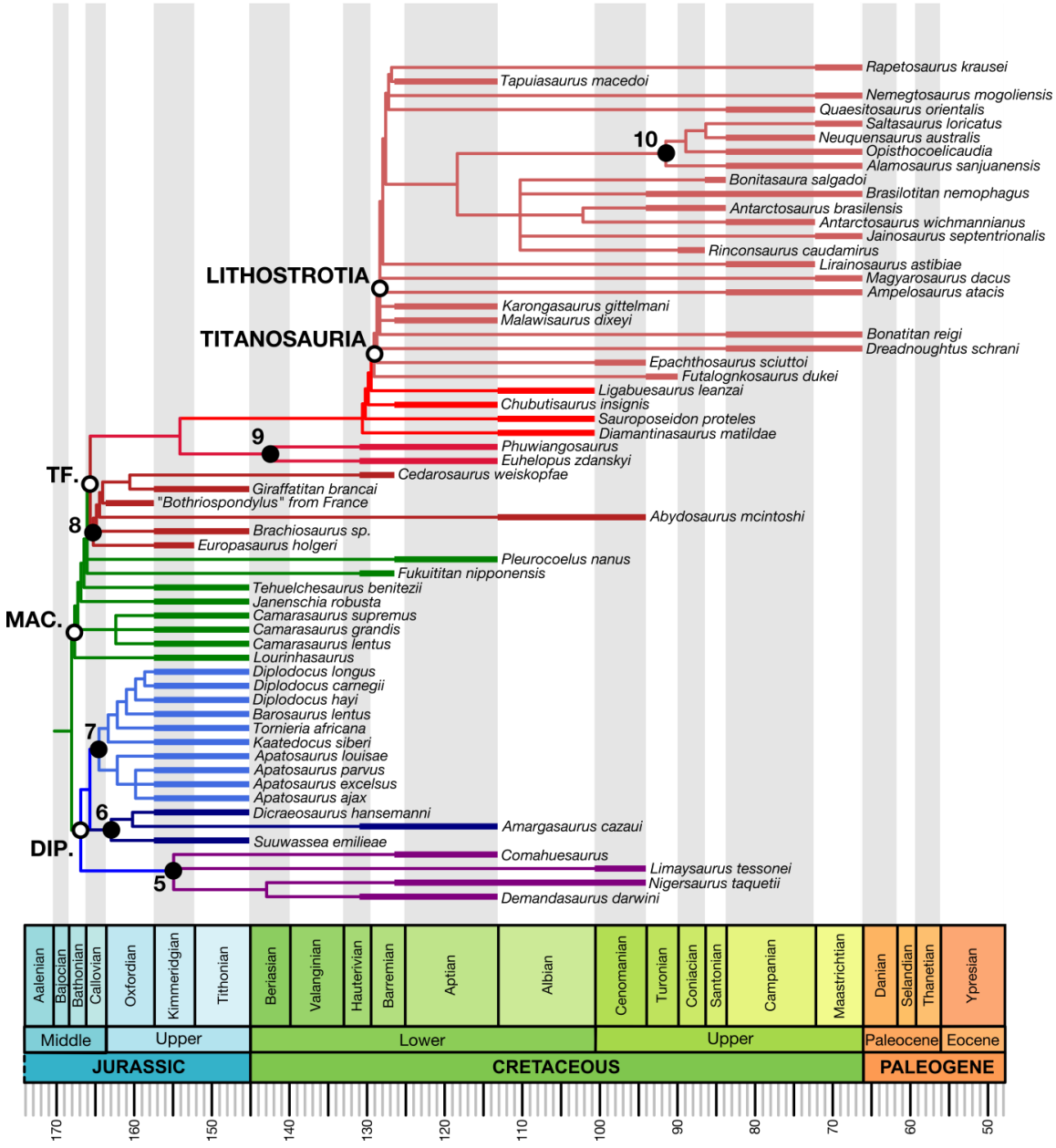

Figure S20: Neosauropod topology of the informal supertree used in this study, based primarily on Benson *et al.* (2014) (see text). Taxa are DIP. – Diplodocoidea; MAC. – Macronaria; TF. – Titanosauriformes. Numbered nodes refer to the following families: 5 – Rebbachisauridae; 6 – Dicraeosauridae; 7 – Diplodocidae; 8 – Brachiosauridae; 9 – Euhelopidae; 10 – Saltasauridae. Tree plotted using the Strap package (Bell & Lloyd, 2015) in R.

S6. Craniodental evolution analyses

Scores of taxa on the first two pc axis scores (together accounting for >50% of the total variance) were modelled as continuous characters in analyses of trait evolution. These were mapped onto 1000 randomly resolved and dated trees, pruned to only contain taxa known from PC data. In order to compare the evolution of craniodental biomechanical characters with the results of Benson *et al*. (2014) on the mode of evolution of body mass, the following models were then fitted across these trees, using the "fitContinuous" function of the Geiger R package (Harmon *et al*. 2008):

Brownian motion (BM): a model where trait divergence is a result only of drift according to a random walk. Univariate Brownian motion was taken as the null model, against which other models were tested.

Ornstein-Uhlenbeck (OU), or Hanson, model: unlike BM, an OU model includes both drift and selection. OU models fit a random walk with attraction towards an optimum value (Felsenstein 1988; Hansen 1997; Butler & King 2004). In microevolutionary studies such a model is taken as evidence of stabilization selection about a common adaptive peak, whereas in macroevolutionary scenarios it is instead seen as stabilization within a common adaptive zone (*sensu* Simpson [1944]) (Hunt & Carrano 2010; Ingram & Mahler 2013; Mahler *et al*. 2013). The value α is proportional to the strength of the attraction towards this optimum, a value of 0 (no attraction) will refer simply to Brownian motion (Butler & King 2004). Model performance was compared using the size-corrected Akaike information criterion (AICc).

Early burst (EB) (Harmon *et al*. 2010; see also Blomberg *et al*. 2003 & Freckleton & Harvey 2006): this models the rate of evolution as time dependant, decreasing exponentially through time (Harmon *et al*. 2010). This model is was designed to test for the presence of adaptive radiations *sensu* Simpson (1944, 1953), where the majority of differentiation in a character will

598 occur early within a clade's history, with rates then slowing as niches are filled (Simpson 1944;
599 Foote 1994; Schluter 2000; Blomberg *et al*. 2003; Harmon *et al*. 2010).

600 Lambda (Pagel 1999): Pagel (1999) introduced λ as a measure of character covariance with
601 phylogeny, in order to control for the non-independence of taxa (see also Pagel 1994;
602 Freckleton *et al*. 2002). Values range between 0 and 1, providing a measure of the phylogenetic
603 signal in the character(s); values of 0 refer to complete phylogenetic independence, whereas a
604 value of 1 refers to variance as expected from a random walk over the given tree topology,
605 equivalent to a single-rate Brownian motion model (Pagel 1999).

606 Delta (Pagel 1999): similar to the EB model, this provides a measure of how evolutionary rate
607 has varied through the history of a clade. Node depths are raised to the power of delta; values
608 <1 refer to diversification in the trait(s) being concentrated early on in the history of the clade,
609 whereas values >1 mean that diversification has been concentrated more recently (Pagel 1999).

610 The Kappa model (Pagel 1999) was not fitted to trees due to the ambiguity of interpreting such
611 a model in fossil datasets (Harmon *et al*. 2008).

612 Full results from fitting these models are given in supplementary data SD2.

613 Full results from fitting of multiple evolutionary rate models utilizing the transformPhylo.ML
614 function of the 'Motmot' package are given in supplementary data SD3.

615 **S7. Body mass data**

616 Body mass estimates were taken from Benson *et al*. (2014), where they were calculated from
617 stylopodial circumferences using the scaling relationship of Campione & Evans (2012). Mass
618 estimates were added for the following taxa utilizing the same regression (Campione & Evans,
619 2012), based on published stylopodial dimensons: *Thecodontosaurus antiquus* (Benton *et al*.,
620 2000), *Coloradisaurus brevis* (Apaldetti *et al*., 2013), *Mussaurus patagonicus* (Otero & Pol,

621 2013), *Aardonyx celestae* (Yates *et al*., 2010), *Melanorosaurus readi* (Galton *et al*., 2005),
622 *Lamplughsaura dharmarensis* (Kutty *et al*., 2007), *Tazoudasaurus niami* (Allain & Aquesbi,
623 2008), *Mamenchisaurus jingyangensis* (Zhang *et al*., 1998, with comparison to *M.*
624 *constructus*), *Camarasaurus supremus* (Osborn & Mook, 1921) and *Ampelosaurus atacis* (Le
625 Loeuff, 2005). See supplementary data SD1 for body masses. *Thecodontosaurus*,
626 *Coloradisaurus*, *Mussaurus* and *Aardonyx* were treated as habitual bipeds (Bonnan & Senter,
627 2007; Yates *et al*., 2010; Otero & Pol, 2013; Benson *et al*., 2014), although there is potential
628 for facultative quadrupedalism in these taxa (Yates *et al*., 2010; Benson *et al*., 2014; McPhee
629 *et al*., 2014). The mass estimate reported by Benson *et al*. (2014) for *Camarasaurus lentus* was
630 based upon measurement of a juvenile specimen (CM 11338); here, the mass was re-calculated
631 based upon the dimensions of an adult *C. lentus* (Osborn & Mook, 1921; Carrano, 2006).
632 Finally, the mass estimate for *Dreadnoughtus schrani* calculated by Lacovara *et al*. (2014) was
633 included, it too being derived from the regression of Campione & Evans (2012). This resulted
634 in body mass data for 96 taxa, of which 46 are also represented by PC axis scores. It should be
635 noted that the mass calculations derived from such scaling relationships often differ from those
636 calculated from volumetric reconstructions (Brassey et al., 2015; Bates et al., 2015) and are
637 highly sensitive to ontogenetic stage (Brassey *et al*. 2015). Although infant and young juvenile
638 specimens were omitted, masses derived from subadult material were included for some taxa
639 from which adult material is unknown. In particular, the least massive taxon, *Pantydraco*
640 *caducus*, is known only from immature remains (Yates, 2003; Galton *et al*., 2007). However,
641 inclusion of *Pantydraco* does not significantly increase the total range observed in body mass,
642 with masses calculated from adult specimens of related taxa such as *Pampadromaeus* being
643 similar.

S8. SURFACE additional results

The full list of observed instances of convergence across the 100 trees analyses using SURFACE, with the poorly-known *Tornieria* omitted, is given in table S6. Full results are given in supplementary data SD4.

In addition, a sensitivity analysis was conducted omitting other poorly-known taxa: *Thecodontosaurus*, *Arcusaurus*, "*Kunmingosaurus*", *Chinshakiangosaurus*, *Patagosaurus*, *Atlasaurus*, *Demandasaurus*, *Limaysaurus*, *Amargasaurus*, *Suuwassea*, *Ampelosaurus*, *Karongasaurus*, and *Brasilotitan*. These results in lower overall AICc scores (mean -348.25, mean ΔAICc improvement versus a single optimum OU model 95.4). Results are given in supplementary data SD5. Broad results are similar, with 96% of trees demonstrating a regime shift between the base of the Sauropodiformes and the base of the Sauropoda. A shift is observed in the Neosauropoda in 88% of trees, *Riojasaurus* in 67%, *Camarasaurus* in 38% and Diplodocidae in 39%. Diplodocoids and titanosaur taxa here occupy a common regime in 63% of trees, but this is only a result of independent shifts, rather than plesiomorphic inheritance, in 34%.

Convergent tips/clades	% trees which show convergence
Sauropodiformes-*Riojasaurus*	5
Yunnanosaurus-*Riojasaurus*	23
[*Chuxiongosaurus*+Sauropoda]-[*Pantydraco*+Plateosauria]	1
[*Chuxiongosaurus*+Sauropoda]-[*Efraasia*+Plateosauria]	1
Kunmingosaurus-Sauropodomorpha	1
Kunmingosaurus-Sauropodiformes	2
Sauropoda-*Chinshakiangosaurus*	3
[*Atlasaurus*+Sauropodomorpha]-*Riojasaurus*	17
[*Atlasaurus*+Neosauropoda]-Sauropodiformes	1
Dicraeosauridae-Rebbachisauridae	2
Diplodocidae-*Riojasaurus*	17
Diplodocidae-*Yunnanosaurus*	16
Diplodocinae-*Riojasaurus*	2
Diplodocinae-*Yunnanosaurus*	3
Diplodocus-Macronaria	1
Macronaria-Sauropoda	2
Camarasaurus-[*Mussaurus*+Sauropoda]	2
Camarasaurus-[*Aardonyx*+Sauropoda]	6
Camarasaurus-[*Melanorosaurus*+Sauropoda]	1
Camarasaurus-*Chinshakiagnosaurus*	1
Camarasaurus-[*Chinshakiangosaurus*+Sauropoda]	5
Camarasaurus-Sauropoda	33
Euhelopus-Sauropoda	3
Euhelopus-*Camarasaurus*	3
Titanosauria-Dicraeosauridae	1
Karongasaurus-*Suuwassea*	1

Table S6: List of observed incidences of convergence across the 100 observed trees, with the % of trees in which they are recovered given. Clades are defined on the basal node at which the regime shift is observed. Subsequent shifts mean that this regime may only apply to basally branching members of that clade; convergences are often observed between more nested members of a clade with basal forms (hence why some convergence names appear tautologous). Convergences are listed with the temporally latter occurring taxon first. In incidences where multiple convergences towards the same local optimum was observed, all individual convergences are listed here – e.g., if *Chinshakiangosaurus*, the base of the Sauropoda and *Camarasaurus* all showed a shift towards the same local optimum, the results would be listed as 1 for all of the following: Sauropoda-*Chinshakiagnosaurus*, *Camarasaurus*-Sauropoda and *Camarasaurus*-*Chinshakiangosaurus*. See appendix for the full results.

669 **S9. Supplementary references**

670 Allain, R. & Aquesbi, N. 2008. Anatomy and phylogenetic relationships of *Tazoudasaurus*
671 *naimi* (Dinosauria, Sauropoda) from the late Early Jurassic of Morocco. *Geodiversitas*, **30**,
672 345-424.

673 Anderson, M.J. 2001. A new method for non-parametric multivariate analysis of variance.
674 *Austral Ecology*, **26**, 32-46.

675 Anderson, P.S.L. 2009. Biomechanics, functional patterns, and disparity in Late Devonian
676 arthrodires. *Paleobiology*, **35**, 321-342.

677 Anderson, P.S.L., Friedman, M. Brazeau, M.D. & Rayfield, E.J. 2011. Initial radiation of jaws
678 demonstrated stability despite faunal and environmental change. *Nature*, **476**, 206-209.

679 Anderson, P.S.L., Friedman, M. & Ruta, M. 2013. Late to the table: diversification of tetrapod
680 mandibular biomechanics lagged behind evolution of terrestriality. *Integrative and*
681 *Comparative Biology*, **53**, 283-294.

682 Apaldetti, C., Martínez, R.N., Alcober, O.A. & Pol, D. 2011. A new basal sauropodomorpha
683 (Dinosauria: Saurischia) from Quelbrada del Barro Formation (Marayes-El Carrizal Basin),
684 Northwestern Argentina. *PLoS One* **6**, e26964.

685 Apaldetti, C., Pol, D. & Yates, A. 2013. The postcranial anatomy of *Coloradisaurus brevis*
686 (Dinosauria: Sauropodomorpha) from the Late Triassic of Argentina and its phylogenetic
687 implications. *Palaeontology*, **56**, 277-301.

688 Apaldetti, C., Matínez, R.N., Pol, D. & Souter, T. 2014. Redescription of the skull of
689 *Coloradisaurus brevis* (Dinosauria, Sauropodomorpha) from the Late Triassic Los Colorados
690 Formation of Ischigualasto-Villa Union Basin, northwestern Argentina. *Journal of Vertebrate*
691 *Paleontology*, **34**, 1113-1132.

692 Apesteguía, S. 2007. The sauropod diversity of the La Amarga Formation (Barremian),
693 Neuquén (Argentina). *Gondwana Research*, **12**, 533-546.

694 Barrett, P.M. 2000. Prosauropods and iguanas: speculation on the diets of extinct reptiles. *In*:
695 Sues, H.-D. (*ed*.) *The Evolution of Herbivory in Terrestrial Vertebrates: Perspectives from the*
696 *Fossil Record*. Cambridge University Press, Cambridge, 42–78.

697 Barrett, P.M. & Upchurch, P. 1994. Feeding mechanisms of *Diplodocus*. *Gaia*, **10**, 195-203.

698 Barrett, P.M. & Upchurch, P. 2005. Sauropodomorph diversity through time:
699 macroevolutionary and paleoecological implications. *In:* Curry Rogers, K.A. & Wilson, J.A.
700 (eds.) *The Sauropods: Evolution and Paleobiology*. University of California Press, Berkeley
701 and Los Angeles, California, 125-156.

702 Barrett, P.M. & Upchurch, P. 2007. The evolution of feeding mechanisms in early
703 sauropodomorph dinosaurs. *Special Papers in Palaeontology*, **77**, 91-112.

704 Bates, K.T., Falkingham, P.L., Macaulay, S., Brassey, C. & Maidment, S.C.R. 2015.
705 Downsizing a giant: re-evaluating *Dreadnoughtus* mass. *Biology Letters*, **11**, 20150215.

706 Bell, M.A. & Lloyd, G.., 2014. strap: an R package for plotting phylogenies against
707 stratigraphy and assessing their stratigraphic congruence. *Palaeontology*, **58**, 379-389.

708 Bell, R.H.V. 1971. A grazing ecosystem in the Serengeti. *Scientific American*, **224**, 86-93.

709 Benson, R.B.J., Campione, N.E., Carrano, M.T., Mannion, P.D., Sullivan, C., Upchurch, P. &
710 Evans, D.C. 2014. Rates of dinosaur body mass evolution indicate 170 million years of
711 sustained ecological innovation on the avian stem lineage. *PLoS One*, **12**, e1001853.

712 Benton, M.J., Juul, L., Storrs, G.W. & Galton, P.M. 2000. Anatomy and systematics of the
713 prosauropod dinosaur *Thecodontosaurus antiquus* from the Upper Triassic of southwest
714 England. *Journal of Vertebrate Paleontology*, **20**, 77-108.

715 Blomberg, S.P., Garland, T. & Ives, A.R. 2003. Testing for phylogenetic signal in comparative
716 data: behavioral traits are more labile. *Evolution*, **57**, 717-745.

717 Bonnan, M.F. & Senter, P. 2007. Were the basal sauropodomorph dinosaurs *Plateosaurus* and
718 *Massospondylus* habitual quadrupeds? *In:* Barrett, P.M. & Batten, D.J. (eds.) *Evolution and*
719 *palaeobiology of early sauropodomorph dinosaurs. Special Papers in Palaeontology*, **77**, 139-
720 155.

721 Boue', C. 1970. Morphologie functionnelle des dents labiales chez ruminants. *Mammalia*, **34**,
722 696-711.

723 Brassey, C.A., Maidment, S.C.R. & Barrett, P.M. 2015. Body mass estimates of an
724 exceptionally complete *Stegosaurus* (Ornithischia: Thyreophora): comparing volumetric and
725 linear bivariate mass estimation methods. *Biology Letters*, **11**, 20140984.

726 Brusatte, S.L., Benton, M.J., Ruta, M. & Lloyd, G.T. 2008. Superiority, competition, and
727 opportunism in the evolutionary radiation of dinosaurs. *Science*, **321**, 1485-1488.

728 Butler, M.A. & King, A.A. 2004. Phylogenetic comparative analysis: a modeling approach for
729 adaptive evolution. *The American Naturalist*, **164**, 683-695.

730 Button, D.J., Rayfield, E.J. & Barrett, P.M. 2014. Cranial biomechanics underpins high
731 sauropod diversity in resource-poor environments. *Proceedings of the Royal Society B:*
732 *Biological Sciences*, **281**, 20142114.

733 Cabreira, S.F., Schultz, C.L., Bittencourt, J.S., Soares, M.B., Fortier, D.C., Silva, L.R. &
734 Langer, M.C. 2011. New stem-sauropodomorph (Dinosauria, Saurischia) from the Triassic of
735 Brazil. *Naturwissenschaften*, **98**, 1035-1040.

736 Calvo, J.O. 1994. Jaw mechanics in sauropod dinosaurs. *Gaia*, **10**, 183-193.

737 Campione, N.E. & Evans, D.C. 2012. A universal scaling relationship between body mass and
738 proximal limb bone dimnesions in quadrupedal and terrestrial tetrapods. *BMC Biology*, **10**, 1-
739 21.

740 Carpenter, K. & Tidwell, V. 1998. Preliminary description of a *Brachiosaurus* skull from Felch
741 Quarry 1, Garden Park, Colorado. *Modern Geology*, **23**, 69-84.

742 Carrano, M.T. 2006. Body-size evolution in the Dinosauria. *In:* Carrano, M.T., Gaudin, T.J.,
743 Blob, R.W. & Wible, J.R. (eds.) *Amniote Paleobiology: Perspectives on the Evolution of*
744 *Mammals, Birds and Reptiles*. University of Chicago Press, Chicago, 225-268.

745 Christiansen, P. 1999. On the head size of sauropodomorph dinosaurs: implications for ecology
746 and physiology. *Historical Biology*, **13**, 269-297.

747 Christiansen, P. 2000. Feeding mechanisms of the sauropod dinosaurs *Brachiosaurus*,
748 *Camarasaurus*, *Diplodocus* and *Dicraeosaurus*. *Historical Biology*, **14**, 137-152.

749 Chure, D., Britt, B.B., Whitlock, J.A. & Wilson, J.A. 2010. First complete sauropod dinosaur
750 skull from the Cretaceous of the Americas and the evolution of sauropod dentition.
751 *Naturwissenschaften*, **97**, 379-391.

752 Cuff, A.R. & Rayfield, E.J. 2013. Feeding mechanics in spinosaurid theropods and extant
753 crocodilians. *PLoS One*, **8**, e65295.

754 D’Emic, M.D. 2012. The early evolution of titanosauriform sauropod dinosaurs. *Zoological*
755 *Journal of the Linnean Society* **166**, 624-671.

756 D’Emic, 2013. Revision of the sauropod dinosaurs of the Lower Cretaceous Trinity Group,
757 southern USA, with the description of a new genus. *Journal of Systematic Paleontology*, **11**,
758 707-726.

759 D’Emic, M.D., Whitlock, J.A., Smith, K.M., Fisher, D.C. & Wilson, J.A. 2013. Evolution of
760 high replacement rates in sauropod dinosaurs. *PLoS One*, **8**, e69235.

761 Dompierre, H. & Churcher, C.S. 1996. Premaxillary shape as an indicator of the diet of seven
762 extinct late Cenozoic new world camels. *Journal of Vertebrate Paleontology*, **16**, 141-148.

763 Ezcurra, M.D. 2010. A new early dinosaur (Saurischia: Sauropodomorpha) from the Late
764 Triassic of Argentina: a reassessment of dinosaur origin and phylogeny. *Journal of Systematic*
765 *Palaeontology*, **8**, 371-425.

766 Fanti, F., Cau, A., Hassine, M. & Contessi, M. 2013. A new sauropod dinosaur from the Early
767 Cretaceous of Tunisia with extreme avian-like pneumatization. *Nature Communications*, **4**, 1-
768 7.

769 Felsenstein, J. 1988. Phylogenies and quantitative characters. *Annual Review of Ecology and*
770 *Systematics*, **19**, 445-471.

771 Fernández-Baldor, F.T., Canudo, J.I., Huerta, P., Montero, D., Suberbiola, X.P. & Salgado, L.
772 2011. *Demandasaurus darwini*, a new rebbachisaurid sauropod from the Early Cretaceous of
773 the Iberian Peninsula. *Acta Palaeontologica Polonica*, **56**, 535-552.

774 Foote, M. 1994. Morphological disparity in Ordovician-Devonian crinoids and the early
775 saturation of morphological space. *Paleobiology*, **20**, 320-344.

776 Fraser, D. & Theodor, J.M. 2011. Comparing ungulate dietary proxies using discriminant
777 function analysis. *Journal of Morphology*, **272**, 1513-1526.

778 Freckleton, R.P. & Harvey, P.H. 2006. Detecting non-Brownian trait evolution in adaptive
779 radiations. *PLoS Biology*, **4**, e373.

780 Freckleton, R.P., Harvey, P.H. & Pagel, M. 2002. Phylogenetic analysis and comparative data:
781 a test and review of evidence. **160**, *The American Naturalist*, 712-726.

782 Gallina, P.A. & Apesteguía, S. 2011. Cranial anatomy and phylogenetic position of the
783 titanosaurian sauropod *Bonitasaura salgadoi*. *Acta Palaeontologica Polonica*, **56**, 45-60.

784 Galton, P.M. 1984. Cranial anatomy of the prosauropod dinosaur *Plateosaurus* from the
785 Knollenmergel (Middle Keuper, Upper Triassic) of Germany. I. Two complete skulls from
786 Trossingen/Württ. With comments on the diet. *Geologica et Palaeontologica*, **18**, 139–171.

787 Galton, P.M. 1985a. Cranial anatomy of the prosauropod dinosaur *Plateosaurus* from the
788 Knollenmergel (Middle Keuper, Upper Triassic) of Germany. II. All the cranial material and
789 details of soft-part anatomy. *Geologica et Palaeontologica*, **19**, 119-159.

790 Galton, P.M. 1985b. Diet of prosauropod dinosaurs from the late Triassic and early Jurassic.
791 *Lethaia*, **18**, 105-123.

792 Galton, P.M. & Upchurch, P. 2004. Prosauropoda. *In: In:* Weishampel, D.B., Dodson, P. &
793 Osmólska, H. (eds.) *The Dinosauria*. University of California Press, Berkerly, 232-258.

794 Galton, P.M., Van Heerden, J. & Yates, A.M. 2005. Postcranial anatomy of referred specimens
795 of the sauropodomorph dinosaur *Melanorosaurus* from the Upper Triassic of South Africa. *In:*
796 Tidwell, V. & Carpeneter, K. (eds.) *Thunder Lizards: The sauropodomorph dinosaurs*. Indiana
797 University Press, Bloomington, 1-37.

798 Galton, P.M., Yates, A.M. & Kermack, D. 2007. *Pantydraco* n. gen. for *Thecodontosaurus*
799 *caducus* Yates, 2003, a basal sauropodomorph dinosaur from the Upper Triassic or Lower
800 Jurassic of South Wales, UK. *Neues Jahrbuch für Geologie und Paläontologie –*
801 *Abhandlungen*, **243**, 119-125.

802 Gans, C. 1974. *Biomechanics: An Approach to Vertebrate Biology*. The University of Michigan
803 Press, Ann Arbor, 261pp.

804 García, R.A. & Cerda, I.A. 2010. Dentición de titanosaurios (Dinosauria, Sauropoda) del
805 Cretácico Superior de la Province de Río Negro, Argentina: morfología, inserción y reemplazo.
806 *Ameghiniana*, **47**, 45-60.

807 Gordon, I.J. & Illius, A.W. 1989. Resource partitioning by ungulates on the Isle of Rhum.
808 *Oecologia*, **79**, 383-389.

809 Gorscak, E., O'Connor, P.M., Stevens, N.J. & Roberts, E.M. 2014. The basal titanosaurian
810 *Rukwatitan bisepultus* (Dinosauria, Sauropoda) from the middle Cretaceous Galula Formation,
811 Rukwa Rift Basin, southwestern Tanzania. *Journal of Vertebrate Paleontology*, **34**, 1133-1154.

812 Greaves, W.S. 1995. Functional predictions from theoretical models of the skull and jaws in
813 reptiles and mammals. *In:* Thomason, J.J. (ed.) *Functional Morphology in Vertebrate*
814 *Paleontology*. Cambridge University Press, Cambridge, 99-115.

815 Hammer, Ø., Harper, D.A.T. & Ryan, P.D. 2001. PAST: Palaeontological statistics software
816 package for education and data analysis. *Palaeontologica Electronica*, **4**, 1-4.

817 Hansen, T.F. 1997. Stabilizing selection and the comparative analysis of adaptation. *Evolution*,
818 **51**, 1341-1351.

819 Harmon, L.J., Weir, J.T., Brock, C.D., Glor, R.E. & Challenger, W. 2008. GEIGER:
820 investigating evolutionary radiations. *Bioinformatics*, **24**, 129-131.

821 Harmon, L.J., Losos, J.B., Davies, T.J., Gillespie, R.G., Gittleman, J.L., Jennings, W.B.,
822 Hozak, K.H., McPeek, M.A., Moreno-Roark, F., Near, T.J., Purvis, A., Ricklefs, R.E., Schluter,
823 D., Schulte, J.A. II, Seehausen, O., Sidlauskas, B.L., Torres-Carvajal, O., Weir, J.T. & Mooers,
824 A.Ø. 2010. Early bursts of body size and shape evolution are rare in comparative data.
825 *Evolution*, **64**, 2385-2396.

826 He X.-L., Li, K. & Cai, K.-J. 1988. *The Middle Jurassic Dinosaur fauna from Dashanpu,*
827 *Zigong, Sichuan: Sauropod Dinosaurs. Vol. 4, Omeisaurus tianfuensis.* Sichuan Publishing
828 House of Science and Technology, Chengdu, 143pp. [Chinese with English summary].

829 Hildebrand, M. 1982. *Analysis of Vertebrate Structure: 2nd Edition*. John Wiley & Sons,
830 Hoboken, 654pp.

831 Holliday, C.M. 2009. New insights into dinosaur jaw muscle anatomy. *The Anatomical Record*,
832 **292**, 1246-1265.

833 Holliday, C.M. & Nesbitt, S.J. 2013. Morphology and diversity of the mandibular symphysis
834 of archosauriforms. *Geological Society of London, Special Publications*, **379**, 555-571.

835 Hummel, J. & Clauss, M. 2011. Sauropod feeding and digestive physiology. *In*: Klein, N.,
836 Remes, K., Gee, C.T. & Sander, P.M. (eds.) *Biology of the Sauropod Dinosaurs:*
837 *Understanding the Life of Giants*. Indiana University Press, Bloomington, pp 11-33.

838 Hunt, G. & Carrano, M.T. 2010. Models and methods for analyzing phenotypic evolution in
839 lineages and clades. *In:* Alroy, J. & Hunt, G. (eds.) *Quantitative Methods in Paleobiology, The*
840 *Paleontological Society Papers*, **16**, 245-269.

841 Hylander, W.L. 1984. Stress and strain in the mandibular symphysis of primates: a test of
842 competing hypotheses. *American Journal of Physical Anthropology*, **64**, 1-46.

843 Hylander, W.L. 1985. Mandibular function and biomechanical stress and scaling. *American*
844 *Zoologist*, **25**, 315-330.

845 Ingram, T. & Mahler, D.L. 2013. SURFACE: detecting convergent evolution from
846 comparative data by fitting Ornstein-Uhlenbeck models with stepwise AIC. *Methods in*
847 *Ecology and Evolution*, **4,** 416-425.

848 Iordansky, N.N. 1964. The jaw muscles of the crocodiles and some relating structures of the
849 crocodile skull. *Anatomischer Anzeiger*, **115**, 256-280.

850 Janensch, W. 1929. Die Wirbelsaule der gattung *Dicraeosaurus*. *Palaeontographica*
851 *(Supplement 7)*, **3**, 39-133.

852 Janensch, W. 1935-6. Die Schadel der Sauropoden Brachiosaurus, Barosaurus, und
853 Dicraeosaurus aus den Tendaguru-Schichten-Deutsch-Ostafrikas. Palaeontographica (Suppl 7)
854 **2**, 147-298.

855 Janis, C.M. & Ehrhardt, D. 1988. Correlation of relative muzzle width and relative incisor
856 width with dietary preference in ungulates. *Zoological Journal of the Linnean Society*, **92**, 267-
857 284.

858 Janis, C.M. 1995. Correlations between craniodental morphology and feeding behaviour in
859 ungulates: reciproca illumination between living and fossil taxa. *In:* Thomason, J.J. (ed.)
860 *Functional Morphology in Vertebrate Paleontology*. Cambridge University Press, Cambridge,
861 76-98.

862 Kutty, T.S., Chatterjee, S., Galton, P.M. & Upchurch, P. 2007. Basal sauropodomorphs
863 (Dinosauria: Saurischia) from the Lower Jurassic of India: their anatomy and relationships.
864 *Journal of Paleontology*, **81**, 1218-1240.

865 Lacovara, K.J., Lamanna, M.C., Ibiricu, L.M., Poole, J.C., Schroeter, E.R., Ullman, P.V.,
866 Voegele, K.K., Boles, Z.M., Carter, A.M., Fowler, E.K., Egerton, V.M., Moyer, A.E.,
867 Coughenour, C.L., Schein, J.P., Harris, J.D., Martínez, R.D. & Novas, F.E. 2014. A gigantic,
868 exceptionally complete titanosaurian sauropod dinosaur from southern Patagonia, Argentina.
869 *Scientific Reports*, **4**, 6196.

870 Le Loeuff, J. 2005. Osteology of *Ampelosaurus atacis* (Titanosauria) from southern France.
871 *In:* Tidwell, V. & Carpeneter, K. (eds.) *Thunder Lizards: The sauropodomorph dinosaurs*.
872 Indiana University Press, Bloomington, 115-137.

873 Machado, E.B., Avilla, L.S., Nava, W.R., Campos, D.A. & Kellner, A.W.A. 2013. A new
874 titanosaur sauropod from the Late Cretaceous of Brazil. *Zootaxa*, **3701**, 301-321.

875 MacLaren, J.A., Anderson, P.S.L., Barrett, P.M. & Rayfield, E.J. In press. Herbivorous jaw
876 disparity and its relationship to extrinsic evolutionary drivers. *Paleobiology*, **XX**, XX.

877 Mahler, D.L., Ingram, T., Revell, L.J. & Losos, J.B. 2013. Exceptional convergence on the
878 macroevolutionary landscape in island lizard radiations. *Science*, **341**, 292-295.

879 Mannion, P.D., Upchurch, P., Carrano, M.T. & Barrett, P.M. 2011. Testing the effect of the
880 rock record on diversity: a multidisciplinary approach to elucidating the generic richness of
881 sauropodomorph dinosaurs through time. *Biological Reviews*, **86**, 157-181.

882 Mannion, P.D., Upchurch, P., Barnes, R.N. & Máteus, O. 2013. Osteology of the Late Jurassic
883 Portuguese sauropod dinosaur Lusotitan atalaiensis (Macronaria) and the evolutionary history
884 of basal titanosauriformes. *Zoological Journal of the Linnean Society*, **168**, 98-206.

885 Mardia, K.V. 1978. Some properties of classic multi-dimensional scaling. *Communications in*
886 *Statistics – Theory and Methods, Series A*, **7**, 1233-1241.

887 Martínez, R.N. 2009. *Adeopapposaurus mognai*, gen. et sp. nov. (Dinosauria:
888 Sauropodomorpha), with comments on adaptations of basal Sauropodomorpha. *Journal of*
889 *Vertebrate Paleontology*, **29**, 142-164.

890 Martínez, R.N. & Alcober, O.A. 2009. A basal sauropodomorph (Dinosauria: Saurischia) from
891 the Ischigualasto Formation (Triassic, Carnian) and the early evolution of Sauropodomorpha.
892 *PLoS One*, **4**, e4397.

893 Martínez, R.N., Sereno, P.C., Alcober, O.A., Colombi, C.E., Renne, P.R., Montañez & Currie,
894 B.S. 2011. A basal dinosaur from the dawn of the dinosaur era in southwestern Pangaea.
895 *Science*, **331**, 206-210.

896 Martínez, R.N., Apaldetti, C. & Abelin, D. 2013. Basal sauropodomorphs from the
897 Ischigualasto Formation. *Journal of Vertebrate Paleontology*, **32**, 51-69.

898 McPhee, B.W., Yates, A.M., Choiniere, J.N. & Abdala, F. 2014. The complete anatomy of and
899 phylogenetic relationships of *Antetonitrus ingenipes* (Sauropodiformes, Dinosauria):
900 implications for the origins of the Sauropoda. *Zoological Journal of the Linnean Society*, **171**,
901 151-205.

902 Metzger, K.A., Daniel, W.J.T. & Ross, C.F. 2005. Comparison of beam-theory and finite-
903 element analysis with *in vivo* bone strain data from the alligator cranium. *The Anatomical*
904 *Record*, **283A**, 331-348.

905 Osborn, H.F. & Mook, C.C. 1921. *Camarasaurus*, *Amphicoelias* and other sauropods of Cope.
906 *Memoirs of the American Museum of Natural History, New Series*, **3**, 247-387.

907 Otero, A. & Po,l D. (2013). Postcranial anatomy and phylogenetic relationships of Mussaurus
908 patagonicus (Dinosauria, Sauropodomorpha). *Journal of Vertebrate Paleontology*, **33**, 1138-
909 1168.

910 Pagel, M. 1994. Detecting correlated evolution on phylogenies: a general method for the
911 comparative analysis of discrete characters. *Proceedings of the Royal Society B: Biological*
912 *Sciences*, **255**, 37-45.

913 Pagel, M. 1999. Inferring the historical patterns of biological evolution. *Nature*, **401**, 877-884.

914 Porro, L.B., Holliday, C.M., Anapol, F., Ontiveros, L.C., Ontiveros, L.T. & Ross, C.F. 2011.
915 Free body analysis, beam mechanics, and finite element modeling of the mandible of *Alligator*
916 *mississippiensis*. *Journal of Morphology*, **272**, 910-937.

917 Prieto-Márquez, A. & Norell, M.A. 2011. Redescription of a nearly complete complete skull
918 of *Plateosaurus* (Dinosauria: Sauropodomorpha) from the Late Triassic of Trossingen
919 (Germany). *American Museum Novitates*, **3727**, 1-58.

920 Reisz, R.R. & Sues, H.-D. 2000. Herbivory in late Paleozoic and Triassic terrestrial vertebrates.
921 *In:* Sues, H.-D. (ed.) *Evolution of Herbivory in Terrestrial Vertebrates: Perspectives from the*
922 *Fossil Record*. Cambridge University Press, Cambridge, 9-42.

923 Royo-Torres, R. & Upchurch, P. 2012. The cranial anatomy of the sauropod Turiasaurus
924 riodevensis and implications for its phylogenetic relationships. *Journal of Systematic*
925 *Paleontology*, **10**, 553-583.

926 Sakamoto, M. 2010. Jaw biomechanics and the evolution of biting performance in theropod
927 dinosaurs. *Proceedings of the Royal Society B: Biological Sciences*, **227**, 3327-3333.

928 Salgado, L., Garrido, A., Cocca, S.E. & Cocca, J.R. 2004. Lower Cretaceous rebbachisaurid
929 sauropods from Cerro Aguada del León (Lohan Cura Formation), Neuqén province,
930 northwestern Patagonia, Argentina. *Journal of Vertebrate Paleontology*, **24**, 903-912.

931 Sander, P.M., Christian, A., Clauss, M., Fechner, R., Gee, C.T., Griebeler, E.-M., Gunga, H.-
932 C., Hummel, J., Mallison, H., Perry, S.F., Preuschoft, H., Rauhut, O.W.M., Remes, K., Tütken,
933 T., Wings, O. & Witzel, U. 2011. Biology of the sauropod dinosaurs: the evolution of
934 gigantism. *Biological Reviews*, **86**, 117-155.

935 Schluter, D. 2000. *The ecology of adaptive radiation*. Oxford University Press, Oxford, 296pp.

936 Sereno, P.C. & Wilson, J.A. 2005. Structure and evolution of a sauropod tooth battery. *In:*
937 Curry Rogers, K.A. & Wilson, J.A. (eds.) *The Sauropods: Evolution and Paleobiology*.
938 University of California Press, Berkeley and Los Angeles, California, 157-177.

939 Sereno, P.C., Forster, C.A., Rogers, R.R. & Monetta, A.M. 1993. Primitive dinosaur skeleton
940 from Argentina and the early evolution of Dinosauria. *Nature*, **361**, 64-66.

941 Sereno, P.C., Wilson, J.A., Witmer, L.M., Whitlock, J.A., Maga, A., Ide, O. & Rowe, T.A.
942 2007. Structural extremes in a Cretaceous dinosaur. *PLoS One*, **2**, e1230.

943 Sereno, P.C., Ricardo, N.M. & Alcober, O.A. 2013. Osteology of *Eoraptor lunensis*
944 (Dinosauria: Sauropodomorpha). *Journal of Vertebrate Paleontology*, **32**, 83-179.

945 Simpson, G.G. 1944. *Tempo and Mode in Evolution*. Columbia University Press, New York,
946 237pp.

947 Simpson, G.G. 1953. *The Major Features of Evolution*. Columbia University Press, New York,
948 434pp.

949 Solounias, N. & Moelleken, S.M.C. 1993. Dietary adaptations of some extinct ruminants
950 determined by premaxillary shape. *Journal of Mammalogy*, **74**, 1059-1071.

951 Solounias, N., Teaford, M. & Walker, A. 1988. Interpreting the diet of extinct ruminants: the
952 case of a non-browsing giraffid. *Paleobiology*, **14**, 287-300.

953 Spencer, L.M. 1995. Morphological correlates of dietary proxies using discriminant function
954 analysis. *Journal of Morphology*, **272**, 1513-1526.

955 Stayton, C.T. 2006. Testing hypotheses of convergence with multivariate data: morphological
956 and functional convergence among herbivorous lizards. *Evolution,* **60,** 824-841.

957 Stubbs, T.L., Pierce, S.E., Rayfield, E.J. & Anderson, P.S.L. 2013. Morphological and
958 biomechanical disparity of crocodile-line archosaurs following the end-Triassic extinction.
959 *Proceedings of the Royal Society of London B: Biological Sciences*, **280**, 20131940.

960 Sues, H.-D. 2000. Herbivory in terrestrial vertebrates: an introduction. *In:* Sues, H.-D. (ed.)
961 *Evolution of Herbivory in Terrestrial Vertebrates: Perspectives from the Fossil Record*.
962 Cambridge University Press, Cambridge, 1-8.

963 Throckmorton, G.S. 1976. Oral food processing in two herbivorous lizards, *Iguana iguana*
964 (Iguanidae) and *Uromastix aegyptius* (Agamidae). *Journal of Morphology*, **148**, 363-390.

965 Tornier, G. 1913. Reptilia (Paläontologie). *Handwörterbuch der Naturwissenschaften*, **8**, 337-
966 376.

967 Tschopp, E. & Mateus, O. 2013. The skull and neck of a flagellicaudatan sauropod from the
968 Morrison Formation and its implication for the evolution and ontogeny of diplodocid dinosaurs.
969 *Journal of Systematic Palaeontology*, **11**, 853-888.

970 Tschopp, E., Mateus, O. & Benson, R.B.J. 2015. A specimen-level phylogenetic analysis and
971 taxonomic revision of Diplodocidae (Dinosauria, Sauropoda). *PeerJ*, **3**, e857.

972 Upchurch, P. 1998. The phylogenetic relationships of sauropod dinosaurs. *Zoological Journal*
973 *of the Linnean Society*, **124**, 43-103.

974 Upchurch, P. 1999. The phylogenetic relationships of the Nemegtosauridae. *Journal of*
975 *Vertebrate Paleontology*, **19**, 106-125.

976 Upchurch, P. & Barrett, P.M. 2000. The evolution of sauropod feeding mechanisms. *In:* Sues,
977 H.-D. (ed.) *Evolution of Herbivory in Terrestrial Vertebrates: Perspectives from the fossil*
978 *record*. Cambridge University Press, Cambridge, 79-122.

979 Upchurch, P., Barrett, P.M. & Dodson, P. 2004. Sauropoda. *In:* Weishampel, D.B., Dodson, P.
980 & Osmólska, H. (eds.) *The Dinosauria*. University of California Press, Berkerly, 259-322.

981 Upchurch, P., Barrett, P.M., Zhao, X.-J. & Xu, X. 2007. A re-evaluation of
982 *Chinshakiangosaurus chunghoensis* Ye *vide* Dong 1992 (Dinosauria, Sauropodomorpha):
983 implications for cranial evolution in basal sauropod dinosaurs. *Geological Magazine*, **144**, 247-
984 262.

985 Vogel, S. 2003. *Comparative Biomechanics: Life's Physical World*. Princeton University
986 Press, Princeton, 640pp.

987 Wainwright, P.C. & Richard, B.A. 1995. Predicting patterns of prey use from morphology of
988 fishes. *Environmental Biology of Fishes*, **44**, 97-113.

989 Wainwright, S.A., Briggs, W.D., Currey, J.D. & Gosline, J.M. 1976. *Mechanical Design in*
990 *Organisms*. Edward Arnold Publishers, London, 423pp.

991 Walmsley, C.W., Smits, P.D., Quayle, M.R., McCurry, M.R., Richards, H.S., Oldfield, C.C.,
992 Wroe, S., Clausen, P.D. & McHenry, C.R. 2013. Why the long face? The mechanics of
993 mandibular symphysis proportions in crocodiles. *PLoS One*, **8**, e53873.

994 Westneat, M.W. 1994. Transmission of force and velocity in the feeding mechanisms of labrid
995 fishes (Teleostei, Perciformes). *Zoomorphology*, **114**, 103-118.

996 Westneat, M.W. 2003. A biomechanical model for analysis of muscle force, power output and
997 lower jaw motion in fishes. *Journal of Theoretical Biology*, **223**, 269-281.

998 Whitlock, J.A. 2011a. Inferences of diplodocoid (Sauropoda: Dinosauria) feeding behaviour
999 from snout shape and microwear analyses. *PLoS One*, **6**, e18304.

1000 Whitlock, J.A. 2011b. A phylogenetic analysis of Diplodocoidea (Saurischia: Sauropoda).
1001 *Zoological Journal of the Linnean Society*, **161**, 872-915.

1002 Wilson, J.A. 2005. Redescription of the Mongolian sauropod *Nemegtosaurus mongoliensis*
1003 (Dinosauria: Saurischia) and comments on Late Cretaceous sauropod diversity. *Journal of*
1004 *Systematic Palaeontology*, **3**, 283-318.

1005 Wilson, J.A. & Upchurch, P. 2009. Redescription and reassessment of the phylogenetic
1006 affinities of *Euhelopus zdanskyi* (Dinosauria: Sauropoda) from the Early Cretaceous of China.
1007 *Journal of Systematic Palaeontology*, **7**, 199-239.

1008 Yates, A.M. 2003. A new species of the primitive dinosaur *Thecodontosaurus* (Saurischia:
1009 Sauropodomorpha) and its implications for the systematics of early dinosaurs. *Journal of*
1010 *Systematic Palaeontology*, **1**, 1-42.

1011 Yates, A.M. 2007a. The first complete skull of the Triassic dinosaur *Melanorosaurus* Haughton
1012 (Sauropodomorpha: Anchisauria). *Special Papers in Palaeontology*, **77**, 9-55.

1013 Yates, A.M., Bonnan, M.F., Neveling, J., Chinsamy, A. & Blackbeard, M.G. 2010. A new
1014 transitional sauropodomorph dinosaur from the Early Jurassic of South Africa and the
1015 evolution of sauropod feeding and quadrupedalism. *Proceedings of the Royal Society B:*
1016 *Biological Sciences*, **277**, 787-794.

1017 Young, M.T., Rayfield, E.J., Holliday, C.M., Witmer, L.M., Button, D.J., Upchurch, P. &
1018 Barrett, P.M. 2012. Cranial biomechanics of *Diplodocus* (Dinosauria, Sauropoda): testing
1019 hypotheses of feeding behaviour in an extinct megaherbivore. *Naturwissenschaften*, **99**, 637-
1020 643.

1021 Zaher, H., Pol, D., Carvalho, A.B., Nascimento, P.M., Riccomini, C., Larson, P., Juarez-
1022 Valieri, R., Pires-Domingues, R., da Silva, N.J. Jr & Campos, D.A. 2011. A complete skull of
1023 an Early Cretaceous sauropod and the evolution of advanced titanosaurians. *PLoS One*, **6**,
1024 e16663.

1025 Zhang, Y. & Yang, Z. 1994. *A new complete os-teology of Prosauropoda in Lufeng Basin*
1026 *Yunnon China:* Jinghsanosaurus. Yunnan Publishing House of Science and Technology,
1027 Kunming, 100pp. [Chinese with English summary].

1028 Zhang, Y., Li, K. & Zeng, Q. 1998. A new species of sauropod from the Late Jurassic of the
1029 Sichuan Basin (*Mamenchisaurus jingyanensis* sp. nov). *Journal of the Chengdu University of*
1030 *Technology*, **25**, 61-68.